



Original Research

Design, synthesis and evaluation of 4,7-disubstituted 8-methoxyquinazoline derivatives as potential cytotoxic agents targeting β -catenin/TCF4 signaling pathway

Kaushik Neogi^a, Prashant R. Murumkar^b, Priyanshu Sharma^c, Poonam Yadav^c,
Mallika Tewari^d, Devarajan Karunakaran^c, Prasanta Kumar Nayak^{a,*}, Mange Ram Yadav^{e,*}

^a Department of Pharmaceutical Engineering and Technology, Indian Institute of Technology (Banaras Hindu University), Varanasi, Uttar Pradesh, India

^b Faculty of Pharmacy, The Maharaja Sayajirao University of Baroda, Vadodara, Gujarat, India

^c Department of Biotechnology, Bhupat and Jyoti Mehta School of Biosciences, Indian Institute of Technology Madras, Chennai, Tamil Nadu, India

^d Department of Surgical Oncology, Institute of Medical Sciences, Banaras Hindu University, Varanasi, Uttar Pradesh, India

^e Centre of Research for Development, Parul University, Vadodara, Gujarat, India



ARTICLE INFO

Keywords:

Wnt/ β -catenin signaling
 β -catenin
TCF4
TCF7L2
Quinazolines
Anticancer agents
 β -catenin/TCF4 interaction inhibitors

ABSTRACT

Overactivation of Wnt/ β -catenin signaling by accumulated β -catenin in the nucleus has been shown to play a crucial role in the etiology of cancer. Interaction of β -catenin with Transcription factor 4 (TCF4) is a key step for the activation of Wnt genes in response to upstream signals of the Wnt/ β -catenin pathway. Hence, down regulation of Wnt/ β -catenin signaling or targeting downstream events by selective β -catenin/TCF4 protein–protein interaction inhibitors could be a potential therapeutic strategy against such cancers. In this study structure-based drug design approach was followed to design novel 4,7-disubstituted 8-methoxyquinazoline-based derivatives which could act as potential cytotoxic agents inhibiting the β -catenin/TCF4 protein–protein interactions. Fifteen compounds possessing 4,7-disubstituted 8-methoxyquinazoline scaffold were synthesized. Cytotoxic potential of the synthesised derivatives were determined against constitutively activated β -catenin/TCF4 signaling pathway cancer cells (HCT116 and HepG2) using the sulforhodamine B assay. The most potent compound (**18B**) was selected for detailed biological evaluation. Cell morphology, Hoechst 33342 and Annexin V/PI staining were used to detect apoptosis, while inhibition of cell migration was assessed by in vitro wound healing assay against HCT116 and HepG2 cells. Effect on β -catenin/TCF4 mediated transcriptional activity was assessed by TOPFlash/FOPFlash assay, TCF4 and β -catenin protein expression by immunocytofluorescence, and Wnt target genes (like c-MYC and Cyclin D1) mRNA levels by RT-PCR against HCT116 cells. Cytotoxic potency of the most potential compound (**18B**) against primary human gallbladder cancer cells was also evaluated. The derivatives showed interactions with active site residues of β -catenin and were capable of hindering the TCF4 binding, thereby disrupting β -catenin/TCF4 interactions. Cytotoxic potencies (IC_{50}) of these derivatives ranged from 5.64 ± 0.68 to $23.18 \pm 0.45 \mu\text{M}$ against HCT116 and HepG2 cells respectively. Compound (**18B**), the most potent compound among the series, induced apoptosis and inhibited cell migration against HCT116 and HepG2 cells. Mechanistic studies indicated that compound (**18B**) downregulated β -catenin/TCF4 signaling pathway, β -catenin and TCF4 protein expression, and mRNA levels of c-MYC and Cyclin D1 in HCT116 cells and showed cytotoxicity against primary human gallbladder cancer cells with IC_{50} value of $8.50 \pm 1.44 \mu\text{M}$. Thus, novel 4,7-disubstituted 8-methoxyquinazoline derivatives were identified as potential cytotoxic agents with potencies comparable to that of imatinib mesylate. Compound (**18B**) represents a promising lead molecule as anticancer agent against colon, hepatocellular and gallbladder cancers targeting β -catenin/TCF4 signaling pathway.

* Corresponding authors at: Prasanta Kumar Nayak, Department of Pharmaceutical Engineering and Technology, Indian Institute of Technology (Banaras Hindu University) Varanasi 221 005, Uttar Pradesh. Mange Ram Yadav, Director (R & D), Centre of Research for Development, Parul University, At & P.O. Limda, Waghodia Road, Vadodara-391760, Gujarat, India.

E-mail addresses: pknayak.phe@iitbhu.ac.in (P.K. Nayak), mryadav11@yahoo.co.in (M.R. Yadav).

<https://doi.org/10.1016/j.tranon.2022.101395>

Received 7 November 2021; Received in revised form 15 February 2022; Accepted 9 March 2022

1936-5233/© 2022 The Authors. Published by Elsevier Inc. This is an open access article under the CC BY-NC-ND license (<http://creativecommons.org/licenses/by-nc-nd/4.0/>).

Introduction

Cancer incidences and mortality are rapidly growing worldwide because of exposure to carcinogenic chemicals, pathogenic microorganism, dietary patterns and lifestyle factors [1,2]. Insights into the molecular pathology of cancer have resulted in the development of targeted novel therapeutics for the treatment of cancer. Deregulation of Wnt/ β -catenin signaling has been implicated in cancer initiation, cancer metastasis, and development of cancer stem cells [3–7]. In the activated Wnt signaling state, Wnt binds to Frizzled (FZD) receptor and low density lipoprotein receptor-related proteins (LRP)-5/6 that lead to activation of Dishevelled protein (DVL) [7,8]. The activated DVL binds to cytoplasmic part of FZD and recruits casein kinase-1 α (CK1 α), inhibiting phosphorylation of β -catenin by glycogen synthase kinase-3 β (GSK3 β) [8–10]. As a consequence, the cytoplasmic tail of LRP-5/6 undergoes phosphorylation by GSK3 β and CK1 α to recruit Axin, thereby preventing β -catenin degradation in the cytoplasm [11–13]. The cytoplasmic β -catenin translocates into the nucleus, binds with T cell factor/Lymphoid enhancer factor (TCF/LEF) and transcriptional co-activators such as B-cell lymphoma-9 (BCL9), Pygopus (Pygo), CREB-binding protein (CBP) and p300, which then activate transcription of Wnt target genes [13–15] as shown in Fig. 1. Wnt target genes such as c-MYC [16], Cyclin D1 [17], Survivin [18], c-jun [19], Met [20], fra-1 [19], PPAR δ [21], Msl1 [22], MMPs [23–25], VEGF [26], uPAR [19] and endothelin-1 [27] which are known to play essential roles in several aspects of tumour development such as transformation, cell growth, proliferation, survival, migration, invasion, angiogenesis, and epithelial to mesenchymal transition. In the absence of Wnt, the cytoplasmic adenomatous polyposis coli (APC) protein, Axin, CK1 α and GSK3 β form a degradation complex with β -catenin [7]. The β -catenin in the complex undergoes a series of phosphorylations to become recognizable by β -transducin repeat-containing protein (β -TrCP) of E3 ubiquitin ligase, which promotes the ubiquitination and proteasomal degradation of β -catenin [7,8,13,28,29]. Consequently, in the absence of nuclear β -catenin, TCF/LEF family of transcription factors interact with co-repressors such as transducin-like enhancer of split (TLE)/Groucho (Gro), histone deacetylases (HDAC), and C-terminal binding protein (CtBP) leading to repression of Wnt target genes [7, 8, 13–15].

A great body of literature indicates that over-activation of Wnt/

β -catenin signaling by accumulated β -catenin in the nucleus plays a crucial role in the development of gastrointestinal cancers including colon cancer (CC) [13,30–34], hepatocellular carcinoma (HCC) [35–41] and gallbladder cancer (GBC) [42–48]. The adjuvant chemotherapeutic agents provide minimal benefits to gastrointestinal cancer patients and are also ineffective in eliminating the self-renewing cancer stem cells. Therefore, there is certainly an urgent need to develop more efficacious drug therapies for the treatment of gastrointestinal cancer. Interaction of β -catenin with Transcription factor-4 (TCF4) [also named as transcription factor 7-like 2 (TCF7L2)] is a key step in the activation of Wnt genes in response to upstream signals of this Wnt/ β -catenin pathway [8, 13]. Hence, downregulation of Wnt/ β -catenin signaling or targeting downstream events by selective β -catenin/TCF4 protein–protein interaction inhibitors could be a potential therapeutic strategy against gastrointestinal cancers including CC, HCC and GBC which might be helpful in early and advanced diseased states and overcoming the prevalence of drug resistance.

Previous experimental data has shown that deletion of the first 12 N-terminal residues from TCF4 had only a marginal effect on binding constants [49]. Mutagenesis data on TCF4 Asp16 residue to Ala showed 50-fold reduction in binding constant [49]. Mutagenesis data on β -catenin Asn426, Lys435, Arg469, His470 and Lys508 residues to Ala showed strong reduction in binding with TCF4 in co-immunoprecipitation experiments. These β -catenin residues form polar contacts with TCF4 residues from Asp16 to Ile19 [49,50]. Another experiment showed mutation on TCF4 Ile19 and Phe21 residues to Ala reduced transcriptional levels to ~60 % [51]. So, we focused on β -catenin active binding residues (Hot spot) which interacts with TCF4 residues from Gly13 to Asp23 region for designing of β -catenin/TCF4 protein–protein interaction inhibitors.

Structure-based design has played an important role in drug discovery and development [52–54]. Approved anticancer drugs like imatinib, gefitinib, erlotinib, sorafenib, lapatinib, abiraterone and crizotinib have been discovered based on computational drug design method [55, 56].

Compounds bearing quinazoline scaffold have been successfully exploited in the discovery of lead molecules due to its facile synthetic accessibility, lead-like and drug-like attributes. Quinazoline template also provides huge opportunities in the lead optimization process.

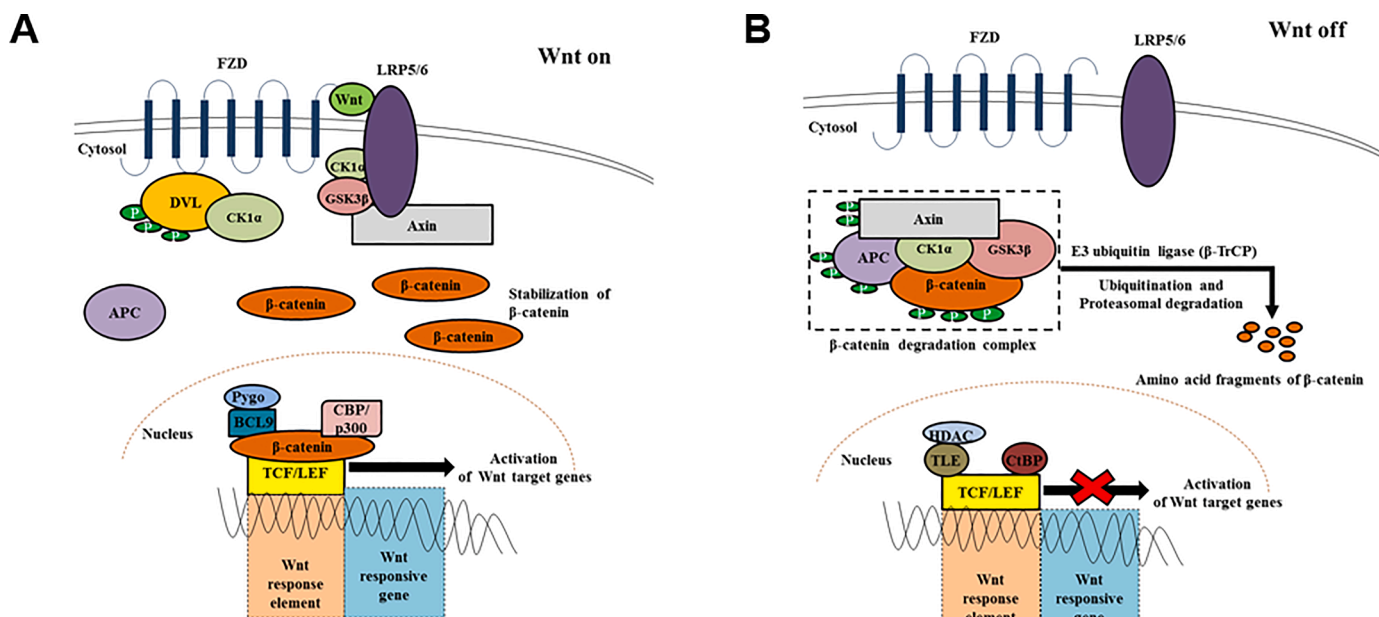


Fig. 1. Wnt/ β -catenin signaling pathway. (A): In the activated Wnt signaling state, β -catenin translocates into the nucleus, binds with T cell factor/Lymphoid enhancer factor (TCF/LEF) and transcriptional co-activators (BCL9, Pygo, CBP/p300) which then activate transcription of Wnt target genes. (B): In the absence of Wnt, TCF/LEF binds to transcriptional co-repressors (TLE, HDAC, CtBP) leading to repression of Wnt target genes.

Introduction of quinazoline molecules such as gefitinib, erlotinib, afatinib, lapatinib and vandetanib as tyrosine kinase inhibitors for the cancer treatment exemplifies some recent successes in optimization of quinazoline lead compounds into clinically useful drugs as shown in Fig. 2A [57–65].

Previous studies have shown that small molecules (I–VIII) (as shown in Fig. 2B) having a quinazoline core proved to be cytotoxic agents that

inhibited the β -catenin/TCF4 pathway [66–70]. All these studies have reported compounds bearing a 2-amino substituent. Some of these compounds are reported to have substituents at 6-/7-position of the quinazoline ring. Taking quinazoline scaffold with substituted amino group at C4 and unsubstituted C2 (similar to anticancer agents having 4-amino quinazoline scaffold approved by the FDA as shown in Fig. 2A) as the lead, we thought of designing and synthesizing quinazoline

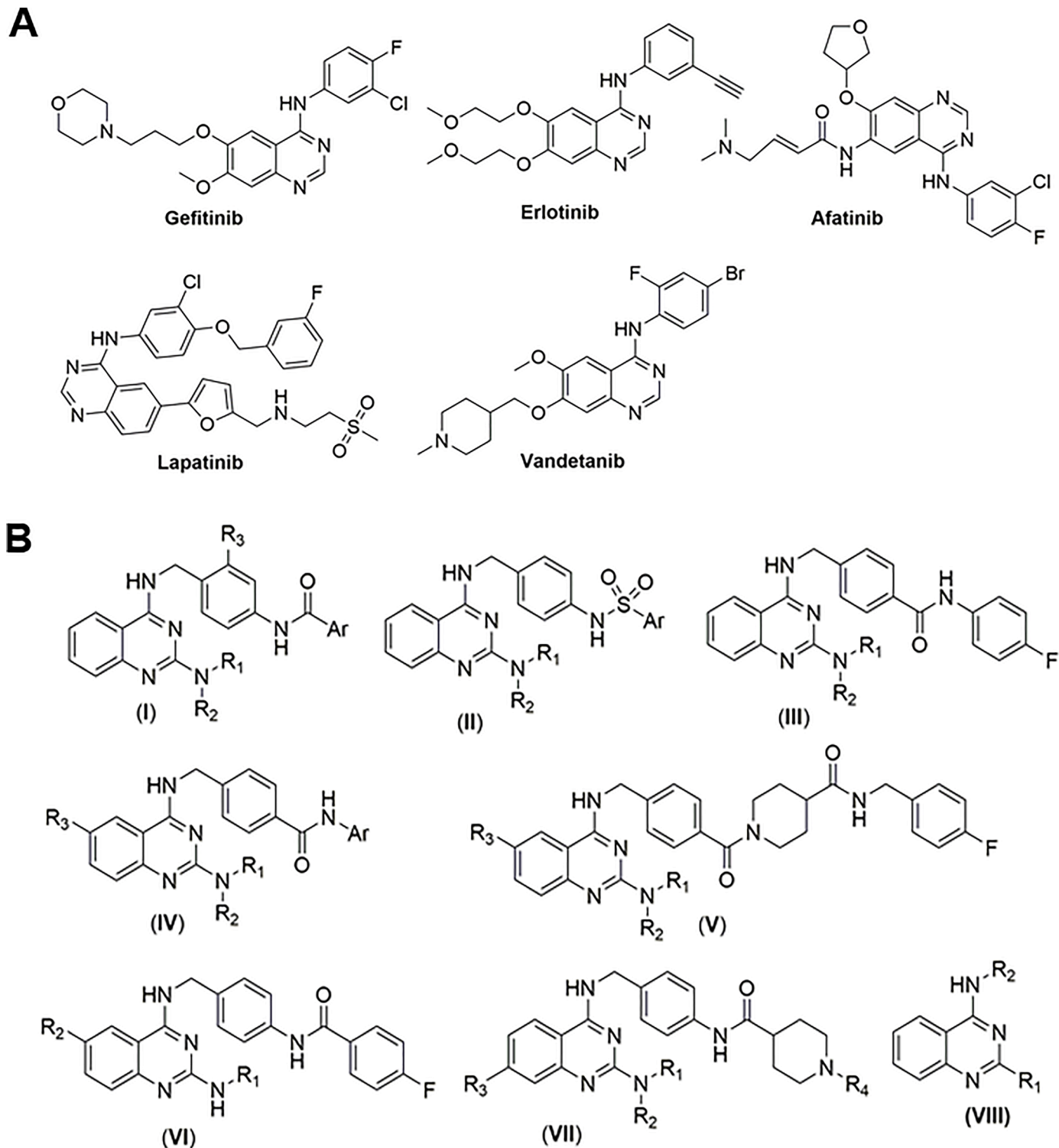


Fig. 2. Quinazoline derivatives as anticancer agents. (A): The structures of some recently developed anticancer agents having 4-amino quinazoline scaffold approved by the Food and Drug Administration (FDA). (B): Previously reported compounds having 4-amino substituent quinazoline core proved to be cytotoxic agents that inhibited the β -catenin/TCF4 pathway.

compounds without a 2-amino substituent but retaining the 4-amino substituent, an aminoalkylether group at position-7 and the methoxyl group at position-8 (as shown in Fig. 3), and assessing these compounds for β -catenin/TCF4 protein–protein interaction inhibition and for anti-cancer activities. It is for the first time that we are reporting these novel compounds.

Thus, some novel compounds containing 4,7-disubstituted 8-methoxyquinazoline core structure were subsequently docked on active binding residues of β -catenin (which interacts with TCF4 from Gly13 to Asp23 region (PDB ID – 2GL7), synthesized, and their cytotoxic potential were evaluated in constitutively activated β -catenin/TCF4 signaling pathway cancer cells (HCT116 and HepG2 cells). The most potent compound was further planned to be examined for anti-carcinogenic activities against HCT116 and HepG2 cells, and for ascertaining the underlying mechanism against HCT116 cells and for cytotoxicity against primary human gallbladder cancer cells.

Materials and methods

Ligand docking using AutoDock 4.2.6

The docking studies were performed using Autodock 4.2.6 [71,72]. The X-ray crystallographic structure of a human β -catenin/TCF4 Complex PDB ID – 2GL7 [73] with a resolution of 2.6 Å was retrieved from Research Collaboratory for Structural Bioinformatics (RCSB) protein data bank (<https://www.rcsb.org/>) in PDB format. Crystallographic water molecules and bound ligands were removed from PDB. The β -catenin protein structure was saved in .pdbqt format by using AutoDockTools (ADT) version 1.5.6 Sep_17_14. The structures of ligands were drawn in ChemDraw Professional version 15.0.0.106. All the structures were then energy-minimized in Chem3D version 15.0.0.106 using MM2 force field and files were saved as .pdb format. By using ADT ligands output files were saved in .pdbqt format. We focused on TCF4 residues from Gly13 to Asp23 region for designing β -catenin/TCF4 protein–protein interaction inhibitors. Arg386, Asn387, Asp390, Thr393, Asn426, Cys429, Asn430, Lys435, Pro463, Cys466, Ala467, Arg469, His470, Ser473, Arg474, Lys508, Arg515, and Asn516 on β -catenin are important active site residues which interacts with TCF4 residues from Gly13 to Asp23 [49, 51, 74-76]. Cubic grid points were set at 112, 114, and 126 along the x, y and z directions respectively for all the ligands with a grid spacing of 0.375 Å. The grid center was set to 19.012, 12.589 and 57.57 Å, respectively. Search parameters were based on using Lamarckian genetic algorithm. The docking was performed using algorithm with 100 runs, 150 population size, 2,500,000 maximum number of energy evaluations and 27,000 maximum number of generations. The Gibbs free binding energy (ΔG) includes vander Waals (ΔG_{vdw}), hydrogen bonding (ΔG_{Hbond}), electrostatic interactions (ΔG_{elec}), torsions (ΔG_{tor}), and desolvation (ΔG_{sol}) were considered for energy based Autodock scoring function. Compounds were subsequently docked on β -catenin (PDB ID – 2GL7) to gain insight into the possible mode of protein ligand interactions at the β -catenin active site. Docking score (Gibbs free binding energy ΔG , estimated in kcal/mol) and predicted inhibitory constant (K_i), were identified by using ADT. Cluster with lowest Gibbs free binding energy was visualized by using DS BIOVIA

Discovery Studio 2016 version 16.1.0 \times 64 for obtaining the binding site interactions.

Synthesis of compounds

All chemicals and solvents were obtained from Merck, Spectrochem, Avra or S.D. Fine Chemical Limited, Mumbai. Solvents were purified and dried by appropriate methods. Aluminium TLC plates pre-coated with GF₂₅₄ silica gel (E. Merck) were used to monitor the reactions. The reported melting points are uncorrected and obtained on Veego (VMP-MP) melting point apparatus. IR spectra were acquired on a Bruker Spectrometer, (model FTIR-8400S). ¹H-NMR (DMSO-*d*₆/) and ¹³C-NMR (CDCl₃) spectra of the synthesized compounds were obtained on Bruker Avance-II 400 NMR Spectrometer. Chemical shifts were measured relative to the internal standard TMS. Chemical shifts are reported in δ scale (ppm). Splitting of the signals is given as broad (b), singlet (s), doublet (d), triplet (t) and multiplet (m). Mass spectra were recorded on ABI MSD Sciex, model API-3000 spectrometer with ESI as an ion source. Purity and composition of the final compounds were determined by elemental analysis, which was found to be within the range of $\pm 0.4\%$ of the calculated values.

4-Hydroxy-3-methoxy-2-nitrobenzoic acid (2)

A solution of 4-acetoxy-3-methoxybenzoic acid(1) [77](2.0 g, 9.5 mM) in glacial acetic acid (6 mL) was cooled over ice-bath in between 10-15°C. A cold mixture of conc. nitric acid (8 mL) and conc. sulphuric acid (6 mL) was added to the above solution drop-wise over a period of 15 minutes. The reaction mixture was stirred at temperature in between 5-10°C for another 1hour and quenched into ice-cold water (50 mL). Precipitate thus formed was filtered, washed with cold water and dried under vacuum to afford 4-hydroxy-3-methoxy-2-nitrobenzoic acid (2) as white solid (1.1 g, 43%), m.p.176-178°C [78]; TLC (R_f): 0.34 (50% Ethyl acetate in hexane); IR: 1692,1554,1377,1170 cm⁻¹.

Methyl 4-hydroxy-3-methoxy-2-nitrobenzoate (3)

To a cold solution of 4-hydroxy-3-methoxy-2-nitrobenzoic acid (2) (2.0 g, 9.38 mM) in methanol (10 mL), thionyl chloride (1.36 mL, 18.7 mM) was added. The above reaction mixture was refluxed under anhydrous conditions for 4hours and quenched into ice-cold water (50 mL). Precipitate thus formed was filtered, washed with cold water and dried to get methyl 4-hydroxy-3-methoxy-2-nitrobenzoate (3) as white solid (1.8 g,84.5%), m.p.180-182°C [77]; TLC (R_f): 0.43 (50% Ethyl acetate in hexane); IR: 3408,1685,1550,1350,1060 cm⁻¹.

Methyl 4-(3-chloropropoxy)-3-methoxy-2-nitrobenzoate (4)

To a solution of methyl 4-hydroxy-3-methoxy-2-nitrobenzoate (3) (1.2 g, 5.2 mM) in DMF (7 mL), 1-bromo-3-chloropropane (0.78 mL, 7.9 mM) and potassium carbonate (1.43 g, 10.2 mM) were added. The reaction mixture was stirred at RT for 4 hours and quenched into cold water. Precipitates thus formed were filtered, washed with cold water and dried to afford methyl 4-(chloropropoxy)-3-methoxybenzoate (4) as white solid (1.4 g, 88.7 %) m.p.77-79°C; TLC (R_f): 0.63 (30 % Ethyl acetate in hexane); IR: 1723, 1548, 1377, 1031, 747cm⁻¹.

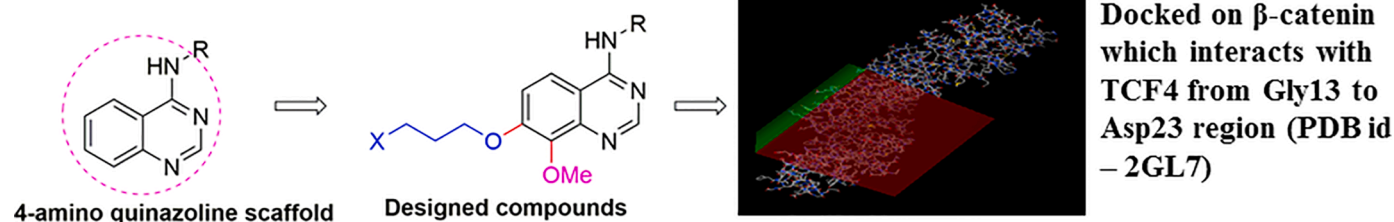


Fig. 3. Designing strategy of the novel 4,7-disubstituted 8-methoxyquinazoline core-containing compounds.

4-(3-Chloropropoxy)-3-methoxy-2-nitrobenzoic acid (5)

Methyl 4-(3-chloropropoxy)-3-methoxy-2-nitrobenzoate (**4**) (2.0 g, 6.58 mM) was dissolved in methanol (15 mL). A solution of potassium hydroxide (1.1 g, 19.7 mM) in water (5.0 mL) was added drop-wise to the above mixture over a period of 20 minutes. The reaction mixture was stirred at RT for another 3 hours and quenched in ice water (200 mL). The precipitates so obtained were filtered and dried under vacuum to afford 4-(3-chloropropoxy)-3-methoxy-2-nitrobenzoic acid (**5**) as white solid (1.70 g, 89.24 %) m.p. 168-170°C; TLC (R_f): 0.31 (30 % Ethyl acetate in hexane); IR: 1692, 1554, 1378, 1044 cm^{-1} .

4-(3-Chloropropoxy)-3-methoxy-2-nitrobenzamide (6)

A solution of 4-(3-chloropropoxy)-3-methoxy-2-nitrobenzoic acid (**5**) (4.0 g, 13.8 mM) in thionyl chloride (4.0 mL) was refluxed under anhydrous conditions for 3 hours in an Rb flask (100 mL). Excess of thionyl chloride was recovered under reduced pressure and the residue was dissolved in THF (20 mL). The above, freshly prepared acid chloride solution was cooled to 5°C and aqueous ammonia solution (4.0 mL) was added to it drop-wise over a period of 15 minutes maintaining the temperature in between 5-10°C. The reaction mixture was stirred for further 4 hours at RT and quenched in cold water (100 mL). Precipitates thus formed were filtered, washed with sodium bicarbonate solution and dried under vacuum to get 4-(3-chloropropoxy)-3-methoxy-2-nitrobenzamide (**6**) as white solid (1.7 g, 85.4 %) m.p. 156-158°C; TLC (R_f): 0.39 (60 % Ethyl acetate); IR: 3366, 3186, 1664, 1622, 1533, 1377, 1048 cm^{-1} .

4-(3-Chloropropoxy)-2-amino-3-methoxybenzamide (7)

A solution of 4-(3-chloropropoxy)-3-methoxy-2-nitrobenzamide (**6**) (1.3 g, 4.5 mM) in methanol (200 mL) was refluxed in a two-neck Rb flask (500 mL). Iron powder (2.5 g, 45 mM) and a solution of sodium chloride (0.79 g, 13.5 mM) in water (4-6 mL) were added portion-wise (in 8-10 parts at an interval of every 45 minutes) to the refluxing solution. Refluxing was continued for further 3 hours, filtered while hot through the filtering aid (Hyflosupercel) and additionally washed with hot methanol (2 × 15 mL). The filtrate was concentrated under reduced pressure to remove excess methanol and the concentrated reaction mixture was kept in refrigerator overnight. The precipitates thus formed were filtered and dried under reduced pressure to get 4-(3-chloropropoxy)-2-amino-3-methoxybenzamide (**7**) as light brown solid (1.1 g, 94.5 %) m.p. 189-192°C; TLC (R_f): 0.43 (60% Ethyl acetate in hexane); IR: 3499, 3438, 1655, 1616, 1105 cm^{-1} ; $^1\text{H-NMR}$: 8.18 (s, 2H, NH_2), 8.04-8.02 (d, 1H, ArH), 7.19-7.17 (d, 1H, ArH), 5.11-5.09 (t, 2H, CH_2), 4.72 (s, 3H, O- CH_3), 4.69-4.67 (t, 2H, NH_2), 3.22-3.19 (t, 2H, CH_2) & 2.55-2.51 (t, 2H, CH_2).

7-(3-Chloropropoxy)-8-methoxyquinazolin-4(3H)-one (8)

A solution of 4-(3-chloropropoxy)-2-amino-3-methoxybenzamide (**7**) (1.0 g, 3.87 mM) in formic acid (20 mL) was stirred at 100°C on oil bath for 8 hours. The reaction mixture was cooled, quenched in ice cold water (30 mL) and kept overnight at RT. The precipitates thus formed were filtered and dried under vacuum to get 7-(3-chloropropoxy)-8-methoxyquinazolin-4(3H)-one (**8**) as white solid (0.9 g, 87.37 %) m.p. 174-176°C; TLC (R_f): 0.4 (Ethyl acetate); IR: 1684, 1655, 1613, 1372, 1077, 741 cm^{-1} ; Mass (m/z): 268.9 (M^+).

General Method of preparation of substituted 4-anilino derivatives (9 - 13)

To a solution of 7-(3-chloropropoxy)-8-methoxyquinazolin-4(3H)-one (**8**) (0.5 g, 1.86 mM) in thionyl chloride (4 mL), catalytic amount of DMF (2 drop) was added, cooled to 5°C and the TEA (0.6 mL) was added drop-wise keeping the temperature below 10°C. The above, reaction mixture was refluxed under anhydrous conditions for 75 minutes, dissolved in anhydrous dioxane (30 mL), cooled to 5°C and the required aniline derivative was added to it drop-wise over a period of 10 minutes maintaining the temperature in between 5-10°C. The reaction mixture was stirred for further 2 hours at RT and quenched in ice cold water (30

mL). The precipitate thus formed was filtered and dried under vacuum to afford the desired substituted 4-anilino derivatives (**9 - 13**).

4N-(3-Chlorophenyl)-7-(3-chloropropoxy)-8-methoxyquinazolin-4-amine (9)

white solid (85.7 %) m.p. 200-202°C; TLC (R_f): 0.66 (70 % Ethyl acetate in hexane); IR: 3325, 3002, 2948, 1083, 784 cm^{-1} .

4N-(3-Bromophenyl)-7-(3-chloropropoxy)-8-methoxyquinazolin-4-amine (10)

white solid (76.92 %) m.p. 196-198°C; TLC (R_f): 0.57 (70 % Ethyl acetate in hexane); IR: 3337, 3062, 2945, 1083, 763 cm^{-1} .

4N-(3-Chloro-4-fluorophenyl)-7-(3-chloropropoxy)-8-methoxyquinazolin-4-amine (11)

white solid (85.03 %) m.p. 209-211°C; TLC (R_f): 0.72 (70 % Ethyl acetate in hexane); IR: 3375, 3073, 2946, 1083, 749 cm^{-1} .

4N-[4-(Benzyloxy-3-chloro)phenyl]-7-(3-chloropropoxy)-8-methoxyquinazolin-4-amine (12): white solid (97.7 %) m.p. 168-170°C; TLC (R_f): 0.24 (50 % Ethyl acetate in hexane); IR: 3326, 3120, 2944, 1083, 734 cm^{-1}

4N-[3-Chloro-4-(3-fluorobenzyloxy)phenyl]-7-(3-chloropropoxy)-8-methoxyquinazolin-4-amine (13): white solid (0.76 g, 97.6 %) m.p. 184-186°C; TLC (R_f): 0.46 (50 % Ethyl acetate in hexane); IR: 3339, 3112, 2943, 1084, 782 cm^{-1} .

General method for the preparation of final compounds (14A - 18C)

To a solution of substituted 4-anilino-7-(3-chloropropoxy)-8-methoxyquinazolin-4-amine (**9 - 13**) (0.2 g, 0.52 mM) in DMF (3 mL), the required amine (0.78 mM) and anhydrous potassium carbonate (0.21 g, 1.56 mM) were added. The reaction mixture was stirred at 60°C on oil bath under anhydrous conditions for 12 hours, quenched into cold water (20 mL) and kept in refrigerator for 48 hours. The precipitate thus formed was filtered, dried under reduced pressure and crystallized with ethyl acetate to afford white crystals of the desired amino derivatives (**14A - 18C**).

4N-(3-Chlorophenyl)-7-(3-(4-morpholinyl)propoxy)-8-methoxyquinazolin-4-amine (14A)

(68.18 %) m.p. 180-181°C; TLC (R_f): 0.61 (Methanol); IR: 3168, 1081, 761 cm^{-1} ; $^1\text{H-NMR}$: 8.79 (s, 1H, NH), 7.92-7.12 (m, 7H, ArH), 4.27-4.25 (t, 2H, CH_2), 4.03, (s, 3H, O- CH_3), 3.77 (bs, 4H, CH_2), 2.67-2.65 (t, 2H, CH_2), 2.56 (bs, 4H, CH_2) & 2.12-2.10 (m, 2H, CH_2); MS: m/z 429.15 (M^+). Anal. Calcd for $\text{C}_{22}\text{H}_{25}\text{N}_4\text{O}_3\text{Cl}$: C, 61.61; H, 5.87; N, 13.06. Found: C, 61.87; H, 6.02; N, 12.84%.

4N-(3-Chlorophenyl)-8-methoxy-7-[3-(4-methyl-1-piperazinyl)propoxy]quinazolin-4-amine (14B)

(82.60 %) m.p. 185-187°C; TLC (R_f): 0.25 (Methanol); IR: 3254, 1083, 761 cm^{-1} ; $^1\text{H-NMR}$: 8.11 (s, 1H, ArH), 7.86-7.11 (7H, ArH), 4.24-4.22 (t, 2H, CH_2), 3.89 (s, 3H, O- CH_3), 3.25 (bs, 4H, CH_2), 2.47-2.45 (t, 2H, CH_2), 2.33-2.30 (m, 5H, NCH₃, CH_2) & 1.95-1.93 (m, 2H, CH_2); MS: m/z 442.20 (M^+). Anal. Calcd for $\text{C}_{23}\text{H}_{28}\text{N}_5\text{O}_2\text{Cl}$: C, 62.51; H, 6.39; N, 15.85. Found: C, 62.35; H, 6.56; N, 15.62%.

4N-(3-Chlorophenyl)-8-methoxy-7-[3-(1,2,4-triazol-1-yl)propoxy]quinazolin-4-amine (14C)

(0.18 g, 85.71 %) m.p. 96-98°C; TLC (R_f): 0.77 (Methanol); IR: 3354, 1088, 777 cm^{-1} ; $^1\text{H-NMR}$: 9.69 (s, 1H, NH), 8.58-7.03 (m, 9H, ArH), 4.45-4.43 (t, 2H, CH_2), 4.18-4.16 (t, 2H, CH_2), 3.97 (s, 3H, O- CH_3) & 2.37-2.35 (m, 2H, CH_2); MS: m/z 411.11 (M^+). Anal. Calcd for $\text{C}_{20}\text{H}_{19}\text{N}_6\text{O}_2\text{Cl}$: C, 58.47; H, 4.66; N, 20.45. Found: C, 58.26; H, 4.83; N, 20.19%.

Table 1Active binding residues (Hot spot) on β -catenin which interacts with TCF4 from Gly13 to Asp23 region

β -catenin residue	TCF4 residue	Type of Interaction
Arg386	Asp23	Electrostatic attractive charge
Arg386	Phe21	Hydrophobic Pi-Alkyl
Asn387	Phe21	Carbon hydrogen bond
Asn387	Asp23	Conventional hydrogen bond
Asp390	Lys22	Electrostatic attractive charge
Thr393	Leu18	Hydrophobic
Asn426	Ile19	Conventional hydrogen bond
Asn426	Phe21	Hydrophobic
Cys429	Leu18	Hydrophobic Alkyl
Cys429	Asp16	Hydrophobic
Cys429	Glu17	Conventional hydrogen bond
Asn430	Asp16	Conventional hydrogen bond
Lys435	Asp16	Hydrogen Bond, Electrostatic attractive charge, Salt Bridge
Pro463	Ile19	Hydrophobic
Cys466	Ile19	Hydrophobic Alkyl
Ala467	Ile19	Hydrophobic
Arg469	Asp16	Electrostatic attractive charge
Arg469	Glu17	Electrostatic attractive charge
Arg469	Ala14	Hydrophobic Alkyl
His470	Asp16	Electrostatic Pi-Anion
His470	Glu17	Carbon hydrogen bond
Ser473	Asp16	Electrostatic attractive charge
Arg474	Gly13	Conventional Hydrogen Bond
Arg474	Ala14	Conventional hydrogen bond
Arg474	Asp16	Electrostatic attractive charge
Arg474	Asn15	Carbon Hydrogen Bond
Lys508	Glu17	Hydrogen Bond, Electrostatic attractive charge, Salt Bridge
Arg515	Ala14	Hydrophobic
Arg515	Asn15	Hydrophobic
Asn516	Ala14	Conventional hydrogen bond
Asn516	Asp16	Electrostatic attractive charge
Asn516	Gly13	Carbon hydrogen bond

***N*-(3-Bromophenyl)-8-methoxy-7-[3-(4-morpholinyl)propoxy]-quinazolin-4-amine (15A)**

(0.16 g, 72.72 %) m.p. 179-181°C; TLC (R_f): 0.3 (Methanol); IR: 3255, 1082, 743 cm^{-1} ; $^1\text{H-NMR}$: 8.72 (s, 1H; ArH), 7.98 (s, 1H; ArH), 7.85 (b, 1H; NH), 7.69-7.67 (d, 1H; ArH), 7.62-7.61 (d, 1H; ArH), 7.26-7.17 (m, 3H; ArH), 4.20-4.18 (t, 2H; OCH₂), 4.03 (s, 3H; OCH₃), 3.70-3.69 (m, 4H; CH₂OCH₂), 2.55-2.52 (t, 2H; NCH₂), 2.45 (b, 4H; CH₂NCH₂), 2.05-1.99 (m, 2H; CH₂CH₂CH₂); $^{13}\text{C-NMR}$: 157.34, 154.69, 154.06, 145.46, 143.04, 139.88, 130.17, 127.11, 124.63, 122.50, 120.27, 116.66, 114.94, 110.54, 67.76, 66.95, 61.73, 55.29, 53.71, 26.46; MS: m/z 473.11 (M^+) and 475.08 ($\text{M}+2$)⁺. Anal. Calcd for C₂₂H₂₅N₄O₃Br: C, 55.82; H, 5.32; N, 11.84. Found: C, 55.73; H, 5.46; N, 11.68%.

***4N*-(3-Bromophenyl)-8-methoxy-7-[3-(4-methyl-1-piperazinyl)propoxy]quinazolin-4-amine (15B)**

(78.26 %) m.p. 195-197°C; TLC (R_f): 0.25 (50% Methanol in chloroform); IR: 3247, 1083, 747 cm^{-1} ; $^1\text{H-NMR}$: 8.78 (s, 1H, NH), 8.04-7.27 (7H, ArH), 4.25-4.23 (t, 2H, CH₂), 4.00 (s, 3H, OCH₃), 2.33-2.31 (t, 2H, CH₂), 2.29-2.22 (m, 6H, CH₂), 2.21 (s, 3H, NCH₃) & 2.13-2.09 (m, 2H, CH₂); MS: m/z 486.15 (M^+) and 488.15 ($\text{M}+2$)⁺. Anal. Calcd for C₂₃H₂₈N₅O₂Br: C, 56.79; H, 5.80; N, 14.40. Found: C, 56.53; H, 5.91; N, 14.14%.

***4N*-(3-Bromophenyl)-8-methoxy-7-[3-(1,2,4-triazol-1-yl)propoxy]quinazolin-4-amine (15C)**

(0.16 g, 76.19 %) m.p. 55-57°C; TLC (R_f): 0.74 (50 % Methanol in chloroform); IR: 3360, 1089, 748 cm^{-1} ; $^1\text{H-NMR}$: δ 8.66 (s, 1H; ArH), 8.37 (b, 1H; NH), 8.20 (s, 1H; ArH), 7.94 (b, 1H; ArH), 7.91 (s, 1H; ArH), 7.74 (b, 1H; ArH), 7.59-7.58 (b, 1H; ArH), 7.18-7.12 (m, 2H; ArH), 7.01-6.99 (d, 1H; ArH), 4.41-4.38 (t, 2H; OCH₂), 4.01-3.99 (m, 5H; OCH₃ &

OCH₂), 2.71 (b, 2H; NCH₂), 2.36-2.30; CH₂CH₂CH₂); $^{13}\text{C-NMR}$: 157.55, 154.72, 153.52, 152.11, 145.47, 143.12, 143.04, 139.96, 130.11, 127.12, 124.87, 122.37, 12.56, 117.51, 114.84, 111.06, 65.78, 61.92, 45.96, 29.37; MS: m/z 455.06 (M^+) and 457.07 ($\text{M}+2$)⁺. Anal. Calcd for C₂₀H₁₉N₆O₂Br: C, 52.76; H, 4.21; N, 18.46. Found: C, 52.48; H, 4.43; N, 18.32%.

***4N*-(3-Chloro-4-fluoro)phenyl-8-methoxy-7-[3-(4-morpholinyl)propoxy]quinazolin-4-amine (16A)**

(72.72 %) m.p. 191-193°C; TLC (R_f): 0.128 (Ethyl acetate); IR: 3161, 1088, 777 cm^{-1} ; $^1\text{H-NMR}$: 8.75 (s, 1H, ArH), 7.90-7.15 (6H, ArH), 4.27-4.24 (t, 2H, CH₂), 4.07 (s, 3H, OCH₃), 3.72 (s, b, 4H, CH₂), 2.59-2.57 (t, 2H, CH₂), 2.48 (bs, 4H, CH₂) & 2.07-2.05 (m, 2H, CH₂); MS: m/z 447.16 (M^+). Anal. Calcd for C₂₂H₂₄N₄O₃ClF: C, 59.13; H, 5.41; N, 12.54. Found: C, 59.24; H, 5.22; N, 12.38%.

***4N*-(3-Chloro-4-fluoro)phenyl-8-methoxy-7-[3-(4-methyl-1-piperazinyl)propoxy]quinazolin-4-amine (16B)**

(69.56 %) m.p. 173-175°C; TLC (R_f): 0.18 (50 % Methanol in chloroform); IR: 3260, 1085, 752 cm^{-1} ; $^1\text{H-NMR}$: 8.74 (s, 1H, ArH), 7.92-7.16 (7H, ArH), 4.25-7.23 (t, 2H, CH₂), 4.07 (s, 3H, OCH₃), 2.61-2.59 (t, 2H, CH₂), 2.29 (s, 3H, NCH₃) & 2.08-2.05 (m, 2H, CH₂); MS: m/z 460.17 (M^+). Anal. Calcd for C₂₃H₂₇N₅O₂ClF: C, 60.06; H, 5.92; N, 15.23. Found: C, 59.89; H, 6.29; N, 15.05%.

***4N*-(3-Chloro-4-fluoro)phenyl-8-methoxy-7-[3-(1,2,4-triazol-1-yl)propoxy]quinazolin-4-amine (16C)**

(71.42 %) m.p. 90-92°C; TLC (R_f): 0.78 (Methanol); IR: 3275, 1090, 745 cm^{-1} ; $^1\text{H-NMR}$: 9.72 (s, 1H, NH), 8.60-7.33 (9H, ArH), 7.24-7.22 (t, 1H, ArH), 4.51-4.48 (t, 2H, CH₂), 4.23-4.20 (t, 2H, CH₂), 4.02 (s, 3H, OCH₃) & 2.42-2.39 (m, 2H, CH₂); MS: m/z 429.12 (M^+). Anal. Calcd for C₂₀H₁₈N₆O₂ClF: C, 56.01; H, 4.23; N, 19.60. Found: C, 55.86; H, 4.36; N, 19.49%.

***4N*-[4-(Benzyloxy)-3-chlorophenyl]-8-methoxy-7-[3-(4-morpholinyl)propoxy]quinazolin-4-amine (17A)**

(0.14 g, 72.4 %) m.p. 173-175°C; TLC (R_f): 0.39 (Methanol); IR: 3262, 1115, 1084, 738 cm^{-1} ; $^1\text{H-NMR}$: 8.70 (s, 1H, NH), 7.77-6.95 (11H, ArH), 4.26-4.23 (t, 2H, CH₂), 5.14 (s, 2H, CH₂), 4.11 (s, 3H, OCH₃), 3.72 (bs, 4H, CH₂), 2.59-2.57 (t, 2H, CH₂), 2.48 (bs, 4H, CH₂) & 2.08-2.05 (m, 2H, CH₂); $^{13}\text{C-NMR}$: 157.71, 154.89, 154.03, 145.42, 143.06, 136.46, 132.13, 128.60, 127.13, 124.90, 123.38, 122.07, 116.69, 114.79, 114.41, 110.43, 71.25, 67.77, 66.97, 61.70, 55.31, 53.70, 26.50; MS: m/z 535.14 (M^+). Anal. Calcd for C₂₉H₃₁N₄O₄Cl: C, 65.10; H, 5.84; N, 10.47. Found: C, 64.78; H, 6.12; N, 10.19%.

***4N*-[4-(Benzyloxy)-3-chlorophenyl]-8-methoxy-7-[3-(4-methyl-1-piperazinyl)propoxy]quinazolin-4-amine (17B)**

(79.5 %) m.p. 154-156°C; TLC (R_f): 0.22 (Methanol); IR: 3139, 1076, 735 cm^{-1} ; $^1\text{H-NMR}$: 8.73 (s, 1H, ArH), 7.78-6.96 (11H, ArH), 5.16 (s, 2H, CH₂), 4.25-4.23 (t, 2H, CH₂), 4.07 (s, 3H, OCH₃), 2.61-2.58 (t, 2H, CH₂), 2.32 (bs, 4H, CH₂) 2.29 (s, 3H, NCH₃) 2.08-2.04 (m, 2H, CH₂) 1.79 (bs, 4H, CH₂); $^{13}\text{C-NMR}$: 157.75, 154.86, 145.39, 142.98, 136.46, 132.19, 128.59, 128.02, 127.13, 124.92, 123.34, 122.11, 116.81, 114.73, 114.39, 110.42, 71.23, 67.86, 61.69, 55.04, 54.88, 53.13, 45.97, 29.78; MS: m/z 548.21 (M^+). Anal. Calcd for C₃₀H₃₄N₅O₃Cl: C, 65.74; H, 6.25; N, 12.78. Found: C, 65.48; H, 6.57; N, 12.45%.

***4N*-[4-(Benzyloxy)-3-chlorophenyl]-8-methoxy-7-[3-(1,2,4-triazol-1-yl)propoxy]quinazolin-4-amine (17C)**

(0.13 g, 70.3 %) m.p. 167-169°C; TLC (R_f): 0.6 (50 % Methanol in ethyl acetate); IR (KBr): 3139, 1076, 744 cm^{-1} ; $^1\text{H-NMR}$: 9.54 (s, 1H, NH), 8.52-7.01 (13H, ArH), 5.19 (s, 2H, CH₂), 4.51-4.48 (t, 2H, CH₂), 4.20-4.18 (t, 2H, CH₂), 4.03 (s, 3H, OCH₃) & 2.45-4.41 (m, 2H, CH₂); $^{13}\text{C-NMR}$: 157.70, 154.90, 153.53, 152.25, 151.37, 145.42, 143.63, 143.34, 136.44, 132.05, 128.62, 128.06, 127.15, 124.92, 123.40,

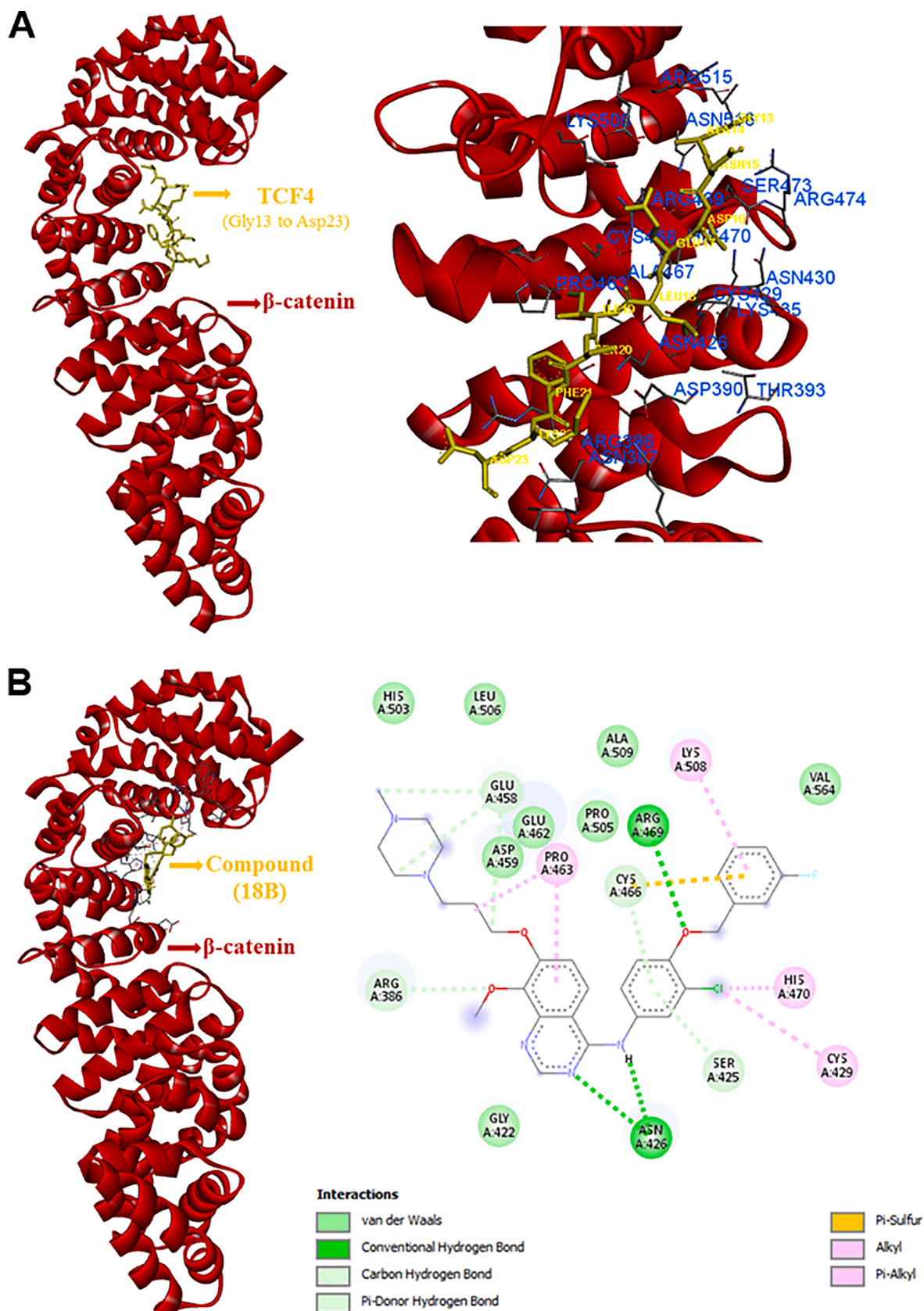


Fig. 4. Structure-based drug design for β -catenin/TCF4 interaction inhibitors. (A): Crystal structure (PDB ID – 2GL7) showing active binding residues (Hot spot) on β -catenin which interacts with TCF4 from Gly13 to Asp23 region. The β -catenin residues are colored blue whereas TCF4 residues are colored yellow. (B): AutoDock predicted binding conformation of compound (18B) on β -catenin (PDB ID – 2GL7).

Table 2

Molecular docking results of 4,7-disubstituted 8-methoxyquinazoline derivatives docked on β -catenin (PDB ID – 2GL7).

Compound	Interacting binding residues on β -catenin	Gibbs free Binding Energy (ΔG in kcal/mole)	Predicted K_i (nM)
14A	Arg386 ^P , Thr418 ^b , Gly422 ^P , Ser425 ^a , Asn426 ^P , Glu458 ^b , Asp459 ^b , Glu462 ^b , Pro463 ⁿ , Pro463 ^o , Cys466 ^g , Cys466 ⁿ , Arg469 ^P , His470 ^P , Pro505 ^P	-7.81	1880
14B	Arg386 ^P , Thr418 ^b , Gly422 ^b , Ser425 ^a , Asn426 ^P , Cys429 ⁱ , Glu458 ^b , Asp459 ^b , Glu462 ^b , Glu462 ^j , Pro463 ^j , Pro463 ⁿ , Pro463 ^o , Cys466 ⁱ , Cys466 ⁿ , Cys466 ^o , Arg469 ^f , His470 ^P , His503 ^P , Pro505 ^P , Lys508 ^P	-8.97	264.6
14C	Thr428 ^P , Cys429 ⁿ , Cys429 ⁿ , Cys429 ^o , Asn430 ^g , Lys435 ^P , Arg469 ^b , Arg469 ^f , Arg469 ⁿ , Arg469 ^o , His470 ^o , Ser473 ^P , Arg474 ^P , Lys508 ⁿ , Lys508 ^o , Val511 ⁿ , Val511 ^o , Gly512 ^P , Arg515 ^b , Arg515 ^f , Arg515 ^o , Asn516 ^b , Glu568 ^P , Ile569 ⁿ , Glu571 ^c , Gly572 ^P	-7.01	7290
15A	Arg386 ^P , Thr418 ^b , Gly422 ^b , Ser425 ^a , Asn426 ^P , Cys429 ⁿ , Glu458 ^b , Glu458 ^P , Asp459 ^b , Glu462 ^b , Pro463 ^h , Pro463 ⁿ , Pro463 ^o , Cys466 ^{g,i} , Arg469 ^f , His470 ^o , His503 ^P , Pro505 ^P , Leu506 ^P	-8.13	1090
15B	Arg386 ^P , Thr418 ^b , Gly422 ^b , Ser425 ^a , Asn426 ^P , Cys429 ⁿ , Glu458 ^b , Asp459 ^b , Glu462 ^b , Pro463 ^h , Pro463 ⁿ , Pro463 ^o , Cys466 ^{g,i} , Arg469 ^f , His470 ^o , His503 ^P , Pro505 ^P , Leu506 ^P	-9.29	154.04
15C	Arg386 ^P , Arg386 ⁿ , Thr418 ^P , Gly422 ^b , Ser425 ^a , Asn426 ^b , Cys429 ⁱ , Glu458 ^a , Glu458 ^c , Asp459 ^e , Glu462 ^e , Pro463 ⁿ , Pro463 ^o , Cys466 ⁿ , Cys466 ^o , Arg469 ^P , His470 ^b , His503 ^P , Pro505 ⁿ	-6.7	12340
16A	Arg386 ^P , Thr418 ^P , Gly422 ^P , Ser425 ^g , Asn426 ^a , Cys429 ⁿ , Glu458 ^P , Asp459 ^b , Glu462 ^b , Pro463 ⁿ , Pro463 ^o , Cys466 ^g , Arg469 ^{a,d} , His470 ^o , His503 ^P , Pro505 ⁿ	-7.61	2650
16B	Arg386 ^P , Thr418 ^b , Gly422 ^P , Ser425 ^a , Asn426 ^P , Cys429 ^{a,c} , Cys429 ⁿ , Glu458 ^b , Asp459 ^b , Pro463 ⁿ , Pro463 ^o , Cys466 ^{g,i} , Arg469 ^f , His470 ^b , His470 ^o , His503 ^P , Pro505 ^P , Leu506 ^P	-8.88	308.12
16C	Thr393 ^b , Lys394 ^b , Lys394 ⁿ , Gln395 ^b , Glu396 ^P , Gly397 ^P , Met398 ^P , Asn430 ^g , Asn431 ^P , Tyr432 ^P , Lys433 ⁿ , Lys433 ^o , Asn434 ^P , Lys435 ^c , Lys435 ⁿ , Met437 ^h , Arg474 ^b , Arg474 ⁿ , His475 ^P	-6.74	11400
17A	Arg386 ^P , Thr418 ^b , Gly422 ^P , Ser425 ^g , Asn426 ^a , Cys429 ⁿ , Glu458 ^b , Asp459 ^b , Glu462 ^c , Pro463 ⁿ , Pro463 ^o , Cys466 ^g , Arg469 ^a , His470 ^o , Pro505 ^P , Lys508 ^f , Lys508 ^o , Ala509 ^o , Val564 ^P	-8.78	369.65
17B	Arg386 ^P , Gly422 ^b , Ser425 ^a , Asn426 ⁿ , Glu458 ^b , Asp459 ^b , Glu462 ^e , Pro463 ^o , Cys466 ⁱ , Cys466 ^o , Arg469 ^{a,c} , His470 ^P	-9.39	130.79

Table 2 (continued)

17C	His503 ^P , Pro505 ^P , Lys508 ^f , Lys508 ^o , Ala509 ^o , Arg469 ^P , Ser473 ^P , Arg474 ^f , Arg474 ^o , His475 ^P , Ala478 ⁿ , Ala478 ^o , Glu479 ^P , Gln482 ^b , Gln482 ^g , Lys508 ^o , Val511 ^o , Gly512 ^P , Arg515 ⁿ , Arg515 ^f , Arg515 ^o , Asn516 ^a , Leu519 ⁿ , Leu519 ^o , Leu519 ^o , Glu568 ^P , Ile569 ^P , Gly572 ^P , Ile579 ^P	-7.19	5350
18A	Arg386 ^P , Thr418 ^P , Gly422 ^a , Gly422 ^b , Ser425 ^g , Asn426 ^P , Glu458 ^P , Asp459 ^b , Glu462 ^P , Pro463 ^o , Cys466 ⁱ , Arg469 ^{a,d} , Pro505 ^P , Lys508 ^b , Lys508 ^o , Ala509 ^o	-8.06	1230
18B	Arg386 ^b , Gly422 ^P , Ser425 ^g , Asn426 ^c , Cys429 ⁿ , Glu458 ^b , Asp459 ^P , Glu462 ^P , Pro463 ⁿ , Pro463 ^o , Cys466 ^g , Cys466 ⁱ , Arg469 ^h , His470 ^o , His503 ^P , Pro505 ^P , Leu506 ^P , Lys508 ^o , Ala509 ^P , Val564 ^P	-9.4	129.57
18C	Arg386 ^P , Gly422 ^b , Ser425 ^a , Asn426 ^P , Cys429 ^o , Glu458 ^b , Asp459 ^P , Glu462 ^e , Pro463 ^h , Pro463 ^o , Cys466 ^{g,i} , Arg469 ^P , His470 ^o , His503 ^P , Pro505 ^o , Leu506 ^P , Lys508 ^f , Lys508 ^o , Ala509 ^o , Val564 ^P	-7.19	5410

a Conventional Hydrogen Bond

b Carbon Hydrogen Bond

c Halogen (Cl, Br, I)

d Halogen (Fluorine)

e Pi-Anion (Electrostatic)

f Pi-Cation (Electrostatic)

g Pi-Donor Hydrogen Bond

h Pi-Sigma (Hydrophobic)

i Pi-Sulfur

j Amide-Pi Stacked (Hydrophobic)

k Pi-Pi Stacked (Hydrophobic),

l Pi-Pi T-shaped (Hydrophobic)

m Pi-Lone Pair

n Alkyl (Hydrophobic)

o Pi-Alkyl (Hydrophobic)

p van der waals

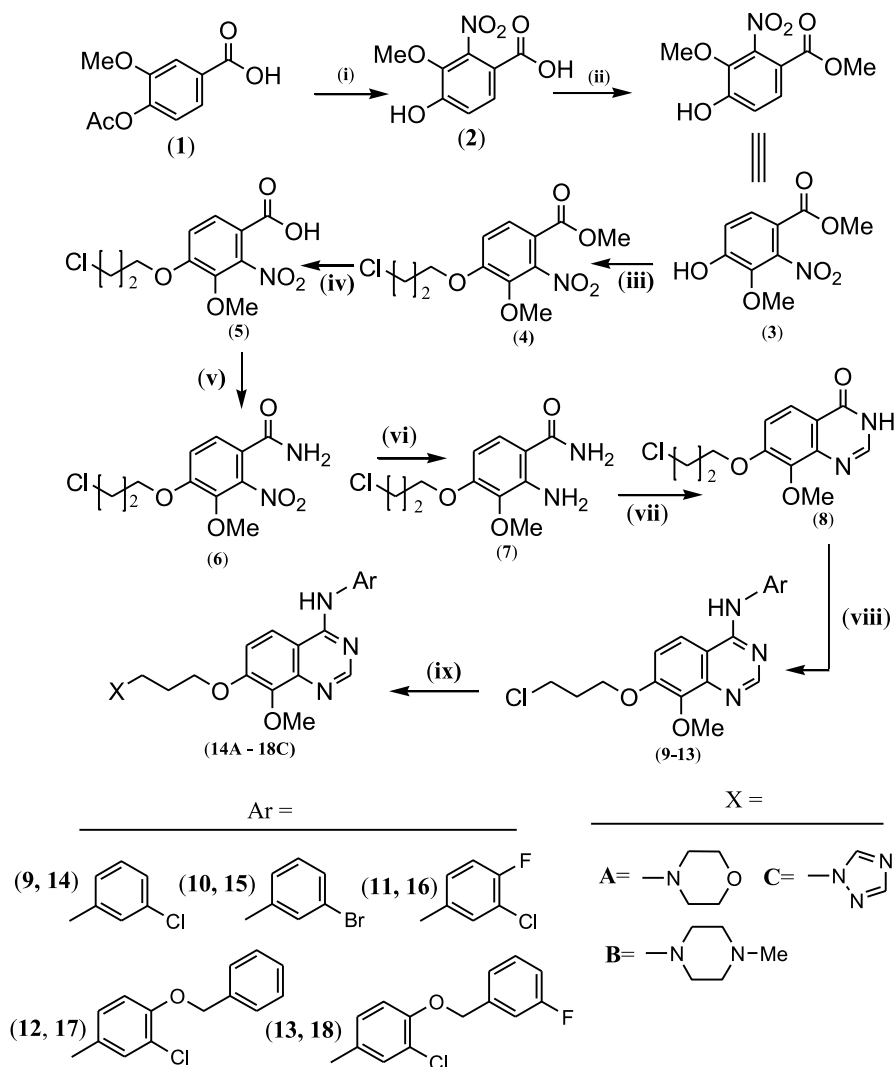
122.09, 117.05, 115.03, 114.42, 110.91, 71.26, 65.88, 61.95, 45.94, 29.42; MS: m/z 517.16 (M^+). Anal. Calcd for $C_{27}H_{25}N_6O_3Cl$: C, 62.73; H, 4.87; N, 16.26. Found: C, 62.45; H, 5.18; N, 15.88%.

4*N*- [3-Chloro-4-(3-fluorobenzoyloxy)phenyl]-8-methoxy-7- [3-(4-morpholinyl)propoxy]- quinazolin-4-amine (18A)

(64.3 %) m.p. 152-154°C; TLC (R_f): 0.55 (50% Methanol in ethyl acetate); IR: 3262, 3145, 1115, 1084, 776 cm^{-1} ; 1H -NMR: 8.73 (s, 1H, NH), 7.75–6.948 (10H, ArH), 5.14 (s, 2H, CH_2), 4.27–4.24 (t, 2H, CH_2), 4.07 (s, 3H, OCH_3), 3.72 (bs, 4H, CH_2), 2.59–2.57 (t, 2H, CH_2) 2.48 (bs, 4H, CH_2) & 2.08–2.04 (m, 2H, CH_2); MS: m/z 553.18 (M^+). Anal. Calcd for $C_{29}H_{30}N_4O_4ClF$: C, 62.98; H, 5.47; N, 10.13. Found: C, 62.61; H, 5.61; N, 9.86%.

4*N*- [3-Chloro-4-(3-fluorobenzoyloxy)phenyl]-8-methoxy-7- [3-(4-methyl-1-piperazinyl)- propoxy]quinazolin-4-amine (18B)

(0.15 g, 68.86 %) m.p. 141-143°C; TLC (R_f): 0.22 (30 % Chloroform in methanol); IR: 3179, 1087, 784 cm^{-1} ; 1H -NMR: 8.73 (s, 1H, NH), 7.77–6.95 (10H, ArH), 5.14 (s, 3H, CH_2), 4.26–4.23 (t, 2H, CH_2), 4.07 (s, 3H, OCH_3), 2.60–2.58 (t, 2H, CH_2), 2.29 (b s, 4H, CH_2), 2.09–2.05 (m, 2H, CH_2) 1.79 (bs, 4H) & 1.25 (s, 3H, NCH_3); MS: m/z 566.01 (M^+). Anal. Calcd for $C_{30}H_{33}N_5O_3ClF$: C, 63.65; H, 5.88; N, 12.37. Found: C, 63.34; H, 6.18; N, 12.13%.



Scheme 1. Reagents and reaction conditions: (i): H_2SO_4 , HNO_3 , AcOH , 10°C , (ii): SOCl_2 , MeOH , refluxing, (iii): 3-Bromochloropropane, DMF , K_2CO_3 , heat, (iv): KOH , MeOH , rt, (v): SOCl_2 , heat followed by addition of aq. NH_3 , (vi): Fe , NaCl , MeOH refluxing, (vii): HCOOH , 100°C , (viii): SOCl_2 , TEA , reflux followed by addition of substituted aniline in dioxane, (ix): Amine (XH) in DMF , 60°C .

4*N*-[3-Chloro-4-(3-fluorobenzyloxy)phenyl]-8-methoxy-7-[3-(1,2,4-triazol-1-yl)propoxy]-quinazolin-4-amine (18C)

(0.11 g, 53.8 %) m.p. $169\text{--}171^\circ\text{C}$; TLC (R_f): 0.7 (70 % Ethyl acetate in hexane); IR: $3257, 1098, 725\text{cm}^{-1}$; $^1\text{H-NMR}$: 9.53 (s, 1H, NH), 8.58–7.27 (12H, ArH), 5.19 (s, 2H, CH_2), 4.52–4.49 (t, 2H, CH_2), 4.20–4.18 (t, 2H, CH_2), 4.03 (s, 3H, OCH_3) & 2.44–4.40 (m, 2H, CH_2); MS: m/z 535.14 (M^+). Anal. Calcd for $\text{C}_{27}\text{H}_{24}\text{N}_6\text{O}_3\text{ClF}$: C, 60.62; H, 4.52; N, 15.71. Found: C, 60.34; H, 4.89; N, 15.49%.

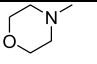
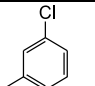
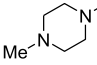
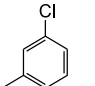
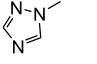
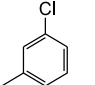
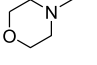
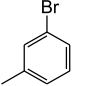
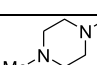
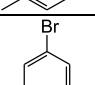
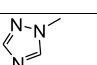
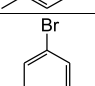
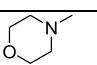
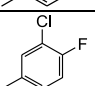
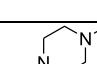
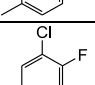
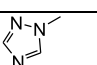
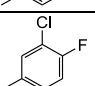
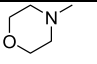
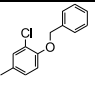
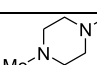
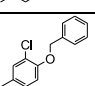
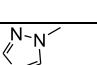
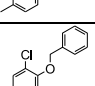
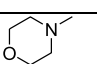
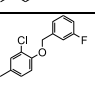
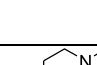
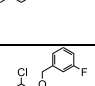
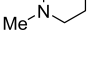
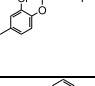
Cell culture

The human colon cancer cell line HCT116 (passage number 24) and human liver cancer cell line HepG2 (passage number 22) were obtained from the National Centre for Cell Science (NCCS), Pune, India. The cells were cultured in Dulbecco's Modified Eagle's medium (DMEM; HiMedia, India) supplemented with 10% v/v fetal bovine serum (FBS; HiMedia, India) and 1% v/v antibiotic antimycotic solution (HiMedia, India). Cells were maintained at 37°C in a humidified 5% CO_2 atmosphere, and growth media were replenished every 48 hours. All the cell lines were tested for mycoplasma contamination through agar-broth culture method and PCR before using them in further experiments.

Cytotoxicity study using Sulforhodamine B assay

Cytotoxic potencies of the synthesised compounds were evaluated in HCT116 and HepG2 cells using the sulforhodamine B assay as described previously with minor modifications [79,80]. Briefly, cells monolayers were trypsinised and 100 μL of cell suspension (5000 cells/well, prepared in media containing 5% v/v FBS) was plated in 96-well plates and incubated for 24 hours to permit recovery from trypsinization. After 24 hours, the medium was aspirated and cells were treated with 200 μL of the test compounds at seven different concentration (0.01, 0.1, 1, 5, 10, 50 and 100 μM)/DMSO (0.5% v/v, served as control) in media containing 5% v/v FBS for 48 hours. Imatinib mesylate (gift sample from Neon Laboratories Limited, Mumbai, India) was used as reference standard. One 96-well plate was kept separately to measure background absorbance for each corresponding wells (wells incubated with growth medium without cells). After incubation with or without test compounds, cells were fixed by the gentle addition of 50 μL of cold 50% w/v Trichloroacetic acid and incubated for 60 minutes at 4°C . The plates were washed four times with tap water by using multichannel pipette and then air dried. SRB solution (0.04% w/v in 1% v/v acetic acid) of 50 μL was added to each of the wells, and plates were incubated for 60 minutes at room temperature. After staining, residual dye was removed by washing four times with 1% v/v acetic acid by using multichannel

Table 3
Cytotoxic effect of 4,7-disubstituted 8-methoxyquinazoline derivatives (14A – 18C) against HCT116 and HepG2 cells

Compound	IUPAC Nomenclature	X	Ar	IC ₅₀ (μM) (Mean ± S.D.)	
				HCT116	HepG2
14A	N-(3-Chlorophenyl)-8-methoxy-7-(3-morpholinylpropoxy)quinazolin-4-amine			11.83 ± 0.85	15.88 ± 0.85
14B	N-(3-Chlorophenyl)-8-methoxy-7-(3-(4-methylpiperazin-1-yl)propoxy)quinazolin-4-amine			12.83 ± 0.65	17.48 ± 0.49
14C	7-(3-(1 <i>H</i> -1,2,4-Triazol-1-yl)propoxy)-N-(3-chlorophenyl)-8-methoxyquinazolin-4-amine			16.18 ± 0.96	20.66 ± 0.53
15A	N-(3-Bromophenyl)-8-methoxy-7-(3-morpholinylpropoxy)quinazolin-4-amine			13.79 ± 0.79	17.72 ± 0.48
15B	N-(3-Bromophenyl)-8-methoxy-7-(3-(4-methylpiperazin-1-yl)propoxy)quinazolin-4-amine			11.86 ± 0.95	15.79 ± 0.73
15C	7-(3-(1 <i>H</i> -1,2,4-Triazol-1-yl)propoxy)-N-(3-bromophenyl)-8-methoxyquinazolin-4-amine			15.62 ± 0.69	19.01 ± 0.51
16A	N-(3-Chloro-4-fluorophenyl)-8-methoxy-7-(3-morpholinylpropoxy)quinazolin-4-amine			17.58 ± 0.64	22.26 ± 0.36
16B	N-(3-Chloro-4-fluorophenyl)-8-methoxy-7-(3-(4-methylpiperazin-1-yl)propoxy)quinazolin-4-amine			11.78 ± 0.79	14.57 ± 0.48
16C	7-(3-(1 <i>H</i> -1,2,4-Triazol-1-yl)propoxy)-N-(3-chloro-4-fluorophenyl)-8-methoxyquinazolin-4-amine			18.70 ± 0.76	21.77 ± 0.71
17A	N-(4-(Benzyloxy)-3-chlorophenyl)-8-methoxy-7-(3-morpholinylpropoxy)quinazolin-4-amine			15.83 ± 0.75	18.30 ± 0.29
17B	N-(4-(Benzyloxy)-3-chlorophenyl)-8-methoxy-7-(3-(4-methylpiperazin-1-yl)propoxy)quinazolin-4-amine			6.51 ± 0.48	9.93 ± 0.89
17C	7-(3-(1 <i>H</i> -1,2,4-Triazol-1-yl)propoxy)-N-(4-(benzyloxy)-3-chlorophenyl)-8-methoxyquinazolin-4-amine			21.74 ± 0.78	23.18 ± 0.45
18A	N-(3-Chloro-4-((3-fluorobenzyl)oxy)phenyl)-8-methoxy-7-(3-morpholinylpropoxy)quinazolin-4-amine			13.47 ± 0.69	16.76 ± 0.27
18B	N-(3-Chloro-4-((3-fluorobenzyl)oxy)phenyl)-8-methoxy-7-(3-(4-methylpiperazin-1-yl)propoxy)quinazolin-4-amine			5.64 ± 0.68	10.97 ± 0.89
18C	7-(3-(1 <i>H</i> -1,2,4-Triazol-1-yl)propoxy)-N-(3-chloro-4-((3-fluorobenzyl)oxy)phenyl)-8-methoxyquinazolin-4-amine			15.43 ± 0.59	18.40 ± 0.73
Imatinibmesylate	4-[(4-Methylpiperazin-1-yl)methyl]-N-(4-methyl-3-{{4-(pyridin-3-yl)pyrimidin-2-yl}amino}phenyl)-benzamidemesylate	-	-	12.98 ± 0.21	16.69 ± 0.38

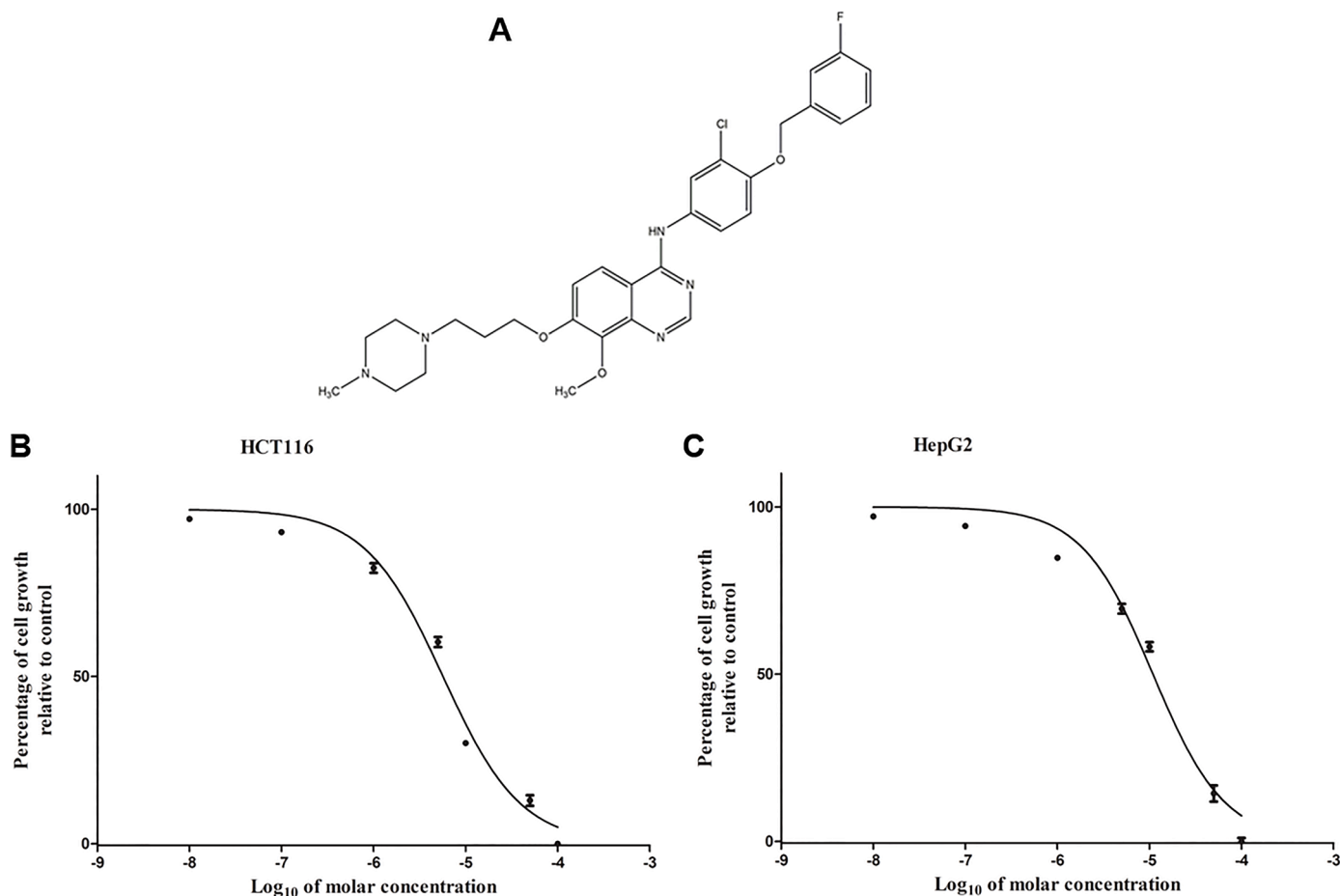


Fig. 5. Concentration response curve of compound (18B) against HCT116 and HepG2 cells. (A): The chemical structure of compound (18B). (B): HCT116 and HepG2 cells were treated with compound (18B) at seven different concentration viz. 0.01, 0.1, 1, 5, 10, 50 and 100 μM for 48 hours and the concentration that caused a 50% reduction in cell growth (IC₅₀) relative to control (0.5% v/v DMSO treated) was determined by the SRB assay. Results are expressed as mean \pm S.D.

pipette and then air dried. Tris base (10mM, pH 10.5) of 100 μL was added to each well and plates were kept on gyratory shaker for 5 minutes to solubilise the dye. Absorbance was read at 490 nm with a microplate-reader (Bio-Rad Laboratories, USA). Background absorbance values were subtracted from all wells. The percentage of cell growth was calculated for each concentration of the test compounds, as [(mean absorbance of wells containing cells treated with test compound)/(mean absorbance of wells containing cells treated with 0.5% v/v DMSO)] \times 100. The concentration that caused a 50% reduction in cell growth (IC₅₀) relative to control (0.5% v/v DMSO treated) was determined by non-linear regression analysis from concentration response curve between concentration versus percentage of cell growth relative to control using GraphPad Prism version 5.01 for Windows (GraphPad Software Inc., USA). Experiments were carried out in triplicate manner.

Cell morphology and Hoechst 33342 staining

HCT116 and HepG2 cells were plated at a density of 1×10^5 cells/well in a 24-well plate and then incubated for 24 hours. After 24 hours, cells were treated with compound (18B) or imatinib mesylate (at IC₅₀ concentration), DMSO (0.5% v/v, served as control) for 48 hours in growth medium containing 5% v/v FBS. After 48 hours, cells bright field microscopic images were captured from inverted microscope (Nikon Ti-U Eclipse, Japan). Then after, the medium was aspirated and washed with Phosphate Buffered Saline (PBS) and then cells were stained with 1 $\mu\text{g}/\text{mL}$ Hoechst 33342 (HiMedia, India) [a fluorescent DNA-staining dye to detect nuclear fragmentation or chromatin condensation, features of apoptosis] for 30 minutes in dark. The morphological changes in the

nucleus stained with Hoechst 33342 were captured from inverted fluorescence microscope (Nikon Ti-U Eclipse, Japan).

Apoptosis determination by Annexin V/PI staining

To examine the effect of compound (18B) on apoptosis induction, HCT116 and HepG2 cells were plated at a density of 2.5×10^5 cells/well in 12-well plate and then incubated for 24 hours. Then after cells were treated with compound (18B) or imatinib mesylate (at IC₅₀ concentration), DMSO (0.5% v/v served as control) for 48 hours in media containing 5% v/v FBS. After 48 hours, cells were harvested and washed with PBS, resuspended in 100 μL of 1x binding buffer and stained with 5 μL Annexin V conjugated Alexa Fluor 488 and 1 μL propidium iodide (PI; 100 $\mu\text{g}/\text{mL}$) for 15 minutes in dark according to the manufacturer's instructions (Thermo Fisher Scientific, #V13241). After incubation period, 300 μL 1x binding buffer was added to each sample before analysis on a BD Accuri C6 Flow cytometer, where Annexin V conjugated Alexa Fluor 488 and PI were detected in the FL-1 and FL-2 channels, respectively. A minimum of 10,000 cells within the gated region was analysed. Data was acquired and analysed using the BD Accuri C6 software (version 1.0.264.21). The results were represented in dot plot, where the lower left (LL) quadrant represented the viable cells (Annexin V⁻, PI⁻), lower right (LR) quadrant represented early apoptotic cells (Annexin V⁺, PI⁻), upper right (UR) quadrant represented late apoptotic cells (Annexin V⁺, PI⁺) and upper left (UL) quadrant represented necrotic cells (Annexin V⁻, PI⁺).

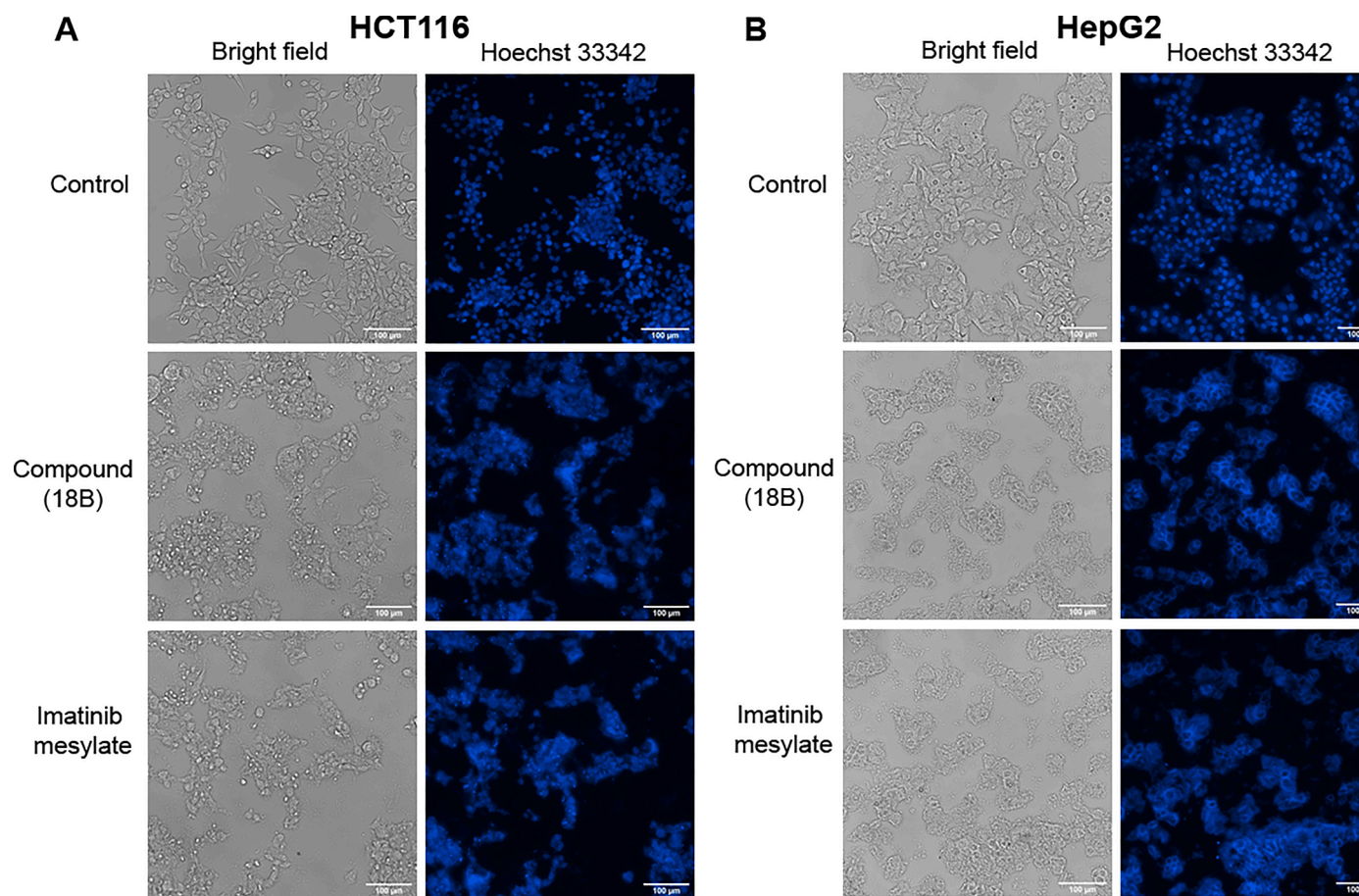


Fig. 6. Effect of compound (18B) on cell morphology and Hoechst 33342 staining of HCT116 and HepG2 cells. (A, B): HCT116 and HepG2 cells were treated with IC₅₀ concentration of compound (18B) or imatinib mesylate for 48 hours. Compound (18B) induced morphological changes like membrane blebbing and cell shrinkage and when stained with Hoechst 33342, nuclear fragmentation and condensation were observed. Magnification 20X and scale bar 100 μ m.

In vitro wound healing (scratch) assay

The scratch assay was performed as described previously with minor modifications [81]. Briefly, HCT116 and HepG2 cells were plated at a density of 5×10^5 cells/well in 6-well plate and then incubated till grown to 80-90% confluency. A scratch was made on the cell monolayer using a 200 μ L sterile pipette tip and the cell debris was removed by washing the cells with PBS. Then the cells were treated with compound (18B) or imatinib mesylate (at IC₅₀ concentration), DMSO (0.5% v/v, served as control) in media containing 5% v/v FBS and bright field microscopic images were captured from inverted microscope (CatScope CS-IB2000, Catalyst Biotech, India) at time zero. Then the cells were incubated for 48 hours and images were taken at each time point to observe the cell migration across the scratch. The percentage of wound area was calculated at each time point using Image J software version 1.53f (Wayne Rasband, National Institutes of Health, USA).

TOPFlash and FOPFlash luciferase reporter assay

A cell-based TOPFlash/FOPFlash assay was done to evaluate the inhibitory effects of candidate inhibitor on β -catenin/TCF mediated transcriptional activity. The HCT116 colon cancer cell line has constitutively activated β -catenin/TCF4 signaling pathway, which can be monitored by a luciferase reporter with TCF4 binding sites in its promoter. Briefly, HCT116 cells were seeded in opaque white 96-well plates (3×10^4 cells/well) and incubated for 24 hours. After 24 hours cells were co-transfected with 100 ng of TOPFlash plasmid (M50 Super 8x

TOPFlash, Addgene plasmid # 12456) or FOPFlash plasmid (M51 Super 8x FOPFlash, Addgene plasmid # 12457) and 10 ng of Renilla luciferase plasmid (pRL-TK, Promega, E2241) constructs using transfection reagent (Lipofectamine® LTX Reagent, Invitrogen) according to the manufacturer's instructions in serum and antibiotic free media. TOPFlash is a luciferase reporter of β -catenin mediated transcriptional activation, with TCF4 binding sites upstream of a luciferase reporter which can specifically measure the activity of β -catenin/TCF4 signal [82]. FOPFlash harbouring mutant TCF4 binding sites upstream of luciferase reporter does not respond to the β -catenin/TCF4 signal. Renilla luciferase served as an internal control for transfection efficiency. After 24 hours of post transfection, the media was aspirated and cells were treated with test compound (18B) or quercetin (at IC₅₀ concentration), DMSO (0.5% v/v served as control) for 24 hours in media containing 5% v/v FBS. Quercetin (Sigma-Aldrich) was used as reference standard. After 24 hours, cells were lysed in 20 μ L 1x passive lysis buffer for 15 minutes and then assayed for dual luciferase activity (TOP or FOP and Renilla) using the Dual-Luciferase® Reporter Assay System (Promega, E1910) according to the manufacturer's instructions. The luminescence reading from each well was measured from Enspire 2300 Multilabel Reader (PerkinElmer). TOP or FOP luciferase activity was normalized to Renilla luciferase activity as a ratio (TOPFlash/Renilla or FOPFlash/Renilla) in order to compensate for variability in transfection efficiencies. Normalized luciferase activity in response to test compound treated cells was compared with DMSO treated cells. Experiments were performed in triplicate.

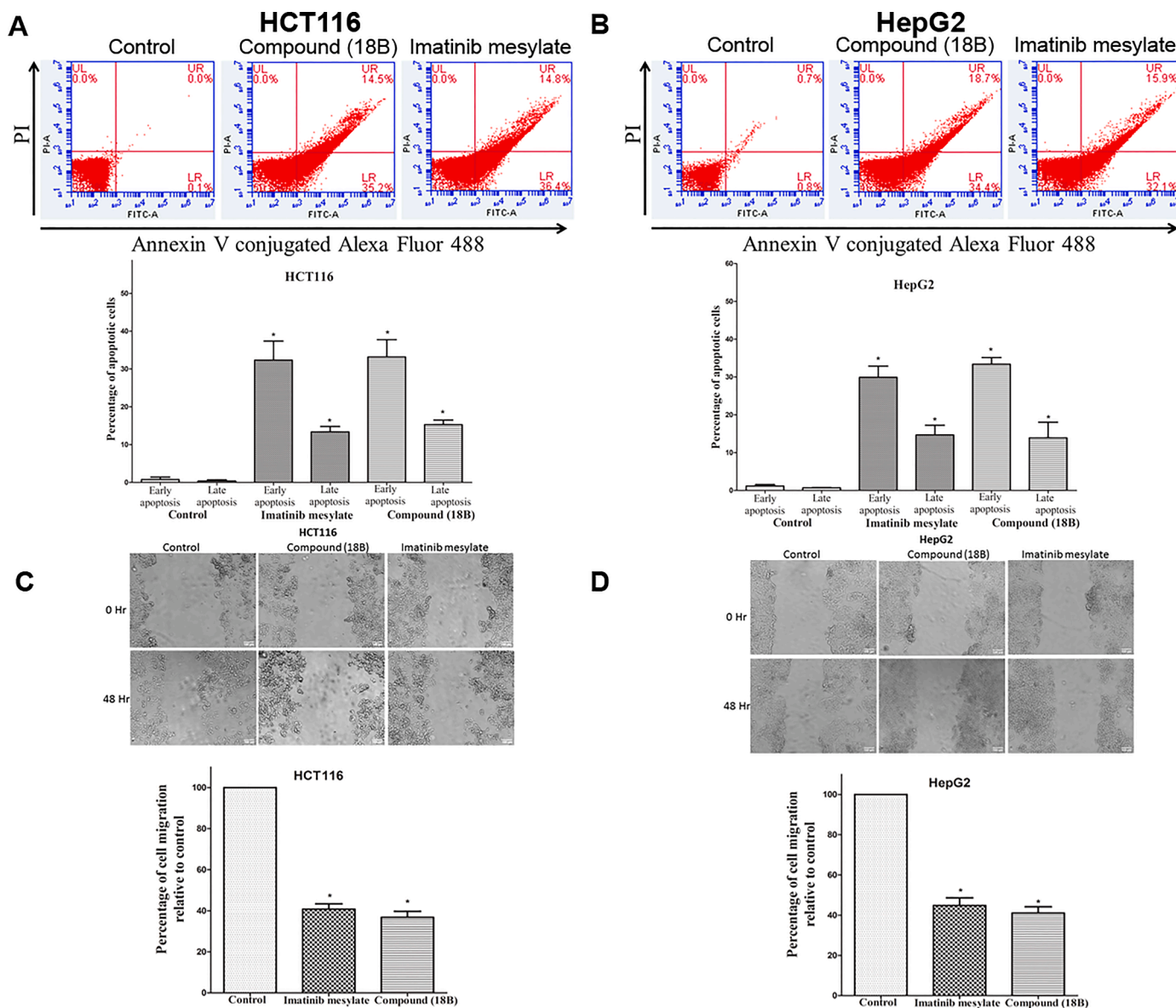


Fig. 7. Effect of compound (18B) on apoptosis and migration of HCT116 and HepG2 cells. Cells were treated with IC₅₀ concentration of compound (18B) or imatinib mesylate for 48 hours. (A, B): Compound (18B) significantly induces apoptosis as compared to control. (C, D): Compound (18B) significantly suppresses the migration as compared to control. Results are expressed as mean ± S.D. * $p < 0.05$ versus control. Magnification 10X and scale bar 100 μ m.

Immunocytofluorescence

The effect of compound (18B) on cellular TCF4/TCF7L2 and β -catenin protein expression was evaluated from immunocytofluorescence. Briefly, HCT116 and HepG2 cells were plated at a density of 1×10^5 cells/well in 24-well plate and then incubated for 24 hours. After 24 hours, cells were treated with test compound (18B) or quercetin (at IC₅₀ concentration), DMSO (0.5% v/v, served as control) for 24 hours in media containing 5% v/v FBS. Then after, the media was aspirated, washed with PBS, cells were fixed with 4% w/v paraformaldehyde in PBS for 15 minutes at room temperature. Fixed cells were washed twice with PBS, permeabilized with 0.2% v/v Triton X-100 in PBS for 15 minutes and blocking was performed with blocking solution (1% w/v BSA, 0.1% v/v Tween 20 in PBS) for 1 hour at room temperature. Then cells were incubated with monoclonal anti-TCF-4 primary antibody, clone 6H5-3 (Upstate, 05-511) or with monoclonal anti- β -catenin primary antibody (Santa Cruz Biotechnology, E-5, Cat.sc-7963) used at 1:200 dilution in blocking solution overnight at 4 °C. After washing with PBS, samples were incubated with Alexa Fluor 546 conjugated goat anti-

mouse IgG (H+L) secondary antibodies (Invitrogen, Cat # A-11003) used at 1:400 dilution in blocking solution for 60 minutes in dark at room temperature and then counterstained with 1 μ g/mL Hoechst 33342 for 30 minutes in dark at room temperature. Microscopic images were captured from inverted fluorescence microscope (Nikon Ti-U Eclipse, Japan). The mean total cell fluorescence was calculated using Image J software version 1.53f (Wayne Rasband, National Institutes of Health, USA).

Reverse transcription polymerase chain reaction (RT-PCR)

The effect of compound (18B) on mRNA levels of c-MYC and Cyclin D1 were quantified by RT-PCR. Briefly, HCT116 and HepG2 cells were plated at a density of 2.5×10^5 cells/well in 12-well plate and then incubated for 24 hours. The cells were treated with compound (18B) or quercetin (at IC₅₀ concentration), DMSO (0.5% v/v served as control) for 24 hours in media containing 5% v/v FBS. Total RNA was extracted from the cell samples using RNAiso Plus (Takara, Cat. #9108). The integrity of total RNA was checked electrophoretically and RNA

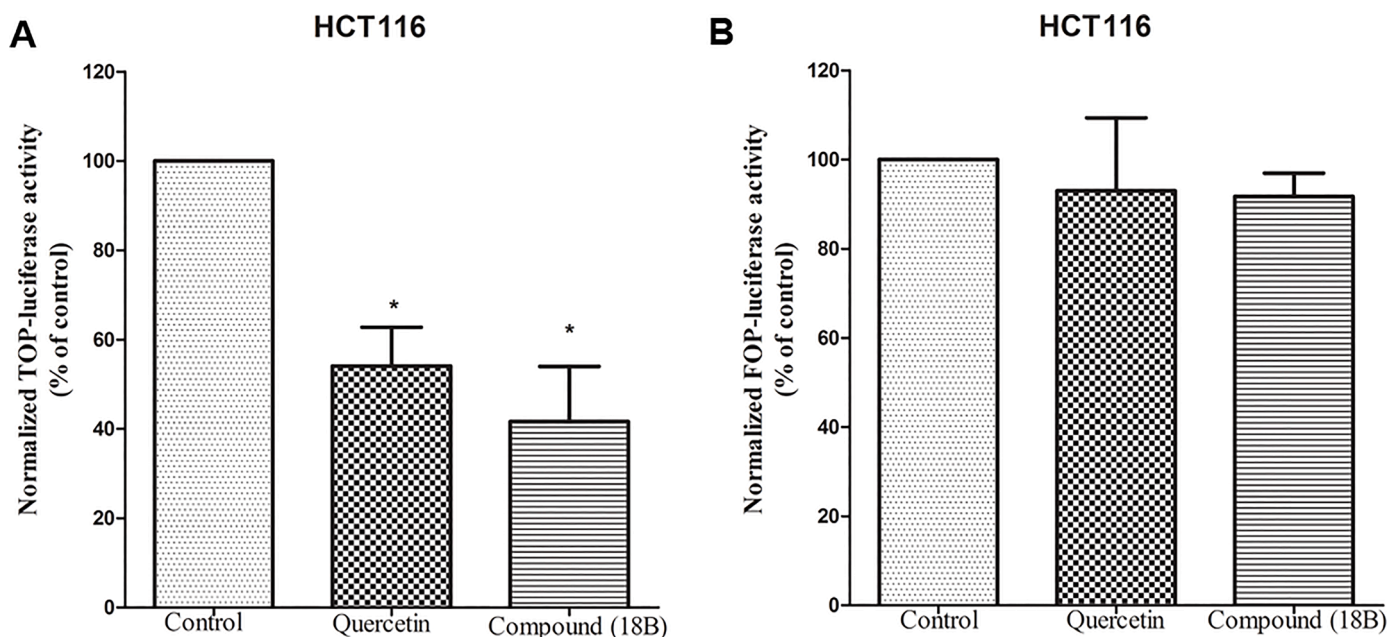


Fig. 8. Effect of compound (18B) on β -catenin/TCF4 signaling pathway. Transfected HCT116 cells were treated with IC₅₀ concentration of compound (18B) or quercetin for 24 hours. (A, B): Compound (18B) significantly reduced TOP-luciferase activity while FOP-luciferase activity remains unaffected indicated that it downregulates β -catenin/TCF4 signaling pathway. Results are expressed as mean \pm S.D. * $p < 0.05$ versus control.

concentration was quantified with a NanoDrop spectrophotometer. Two microgram of total RNA was used for the synthesis of complementary DNA (cDNA) using the cDNA synthesis Kit (Thermo Scientific, #K1622) and amplified using the TopTaq DNA Polymerase (Qiagen, Cat.# 200201) according to the manufacturer's instruction. All primers were analysed using Primer-Blast to ensure primer specificity for the gene of interest (<https://www.ncbi.nlm.nih.gov/tools/primer-blast/>). The primer sequences for c-MYC (Gene ID: 4609) forward 5'-CCTGGTGCTCCATGAGGAGAC-3' and reverse 5'-CAGACTCTGACCTTTTGCCAGG-3'. The primer sequences for Cyclin D1 (Gene ID: 595) forward 5'-TCTACACCGACAACCTCCATCCG-3' and reverse 5'-TCTGGCATTGTTGGAGAGGAAGTG-3'. The primer sequences for reference gene GAPDH (glyceraldehyde 3-phosphate dehydrogenase) (Gene ID: 2597) forward 5'-GTCTCCTCTGACTTCAACAGCG-3' and reverse 5'-ACCACCTGTTGCTGTAGCCAA-3'. The PCR products were run on 1% w/v agarose gel, stained with ethidium bromide (0.5 μ g/mL) and photographed by a BioRad Gel Doc™ EZ (Bio-Rad Laboratories, Hercules, CA, USA). The intensity of bands was noted from Image Lab version 5.2.1 software of BioRad Gel Doc™ EZ.

Evaluation of cytotoxicity in primary human gallbladder cancer cell culture

Surgically resected human gallbladder carcinoma (GBC) tissue of a 60 year old male patient undergoing cholecystectomy was collected at the Department of Surgical Oncology, Institute of Medical Sciences, Banaras Hindu University, Varanasi, India after gaining the approval of the Institutional Ethical Committee of Institute of Science, Banaras Hindu University, Varanasi, India, and informed written consent from the patient. Histologically, the primary tumor was diagnosed as a poorly differentiated adenocarcinoma. We found β -catenin and TCF4/TCF7L2 mRNA levels were overexpressed from RT-PCR study indicating deregulation of Wnt/ β -catenin signaling. Primary human gallbladder cancer cell culture was derived from human GBC tissue specimen. Briefly, tissue sample was washed thrice in PBS containing 1% v/v antibiotic antimycotic solution (HiMedia, India) and then minced into small fragments (1-2 mm) with a scalpel under sterile condition. The chopped pieces were then treated with 0.2% w/v collagenase type I (HiMedia, India),

3mM calcium chloride in PBS and kept at 37°C for 2 hours in an incubator. Then after growth medium (DMEM supplemented with 20% v/v FBS and 1% v/v antibiotic antimycotic solution) was added to stop the proteolytic activity of collagenase. The sample (1,000 rpm, 5 minutes at 4°C) was centrifuged and the pellet was suspended in growth medium and then seeded in T-25 culture flask. Cells were maintained at 37°C in a humidified 5% CO₂ atmosphere in an incubator and grown till 70-80% confluent. Primary cell culture was used to assess drug induced cytotoxicity of compound (18B) and imatinib mesylate in human gallbladder cancer from Sulforhodamine B assay method same as described above.

Statistical analysis

Statistical analysis was performed using GraphPad Prism version 5.01 (GraphPad Software, Inc., USA). Results were compared among more than two groups by one-way analysis of variance followed by Bonferroni's Multiple Comparison Test. Statistical significance was considered at $P < 0.05$.

Results and discussion

The purpose of this study was to design novel quinazoline derivatives which could act as cytotoxic agents with drug-like properties inhibiting the β -catenin/TCF4 protein-protein interactions. It was planned to evaluate cytotoxic potential of these derivatives against constitutively activated β -catenin/TCF4 signaling pathway cancer cells (HCT116 and HepG2). Based on the *in vitro* cytotoxicity data, the most potent compound was to be selected for further biological evaluation. Cell morphology, and Hoechst 33342 and Annexin V/PI staining were planned to be used to detect apoptosis, while inhibition of cell migration was to be assessed by *in vitro* wound healing assay against HCT116 and HepG2 cells. Effect on β -catenin/TCF mediated transcriptional activity was also planned to be assessed by TOPFlash/FOPFlash assay, TCF4 and β -catenin protein expression by immunocytofluorescence, and Wnt target genes (like c-MYC and Cyclin D1) mRNA levels by RT-PCR against HCT116 cells. Cytotoxic potency was to be evaluated against primary human gallbladder cancer cells.

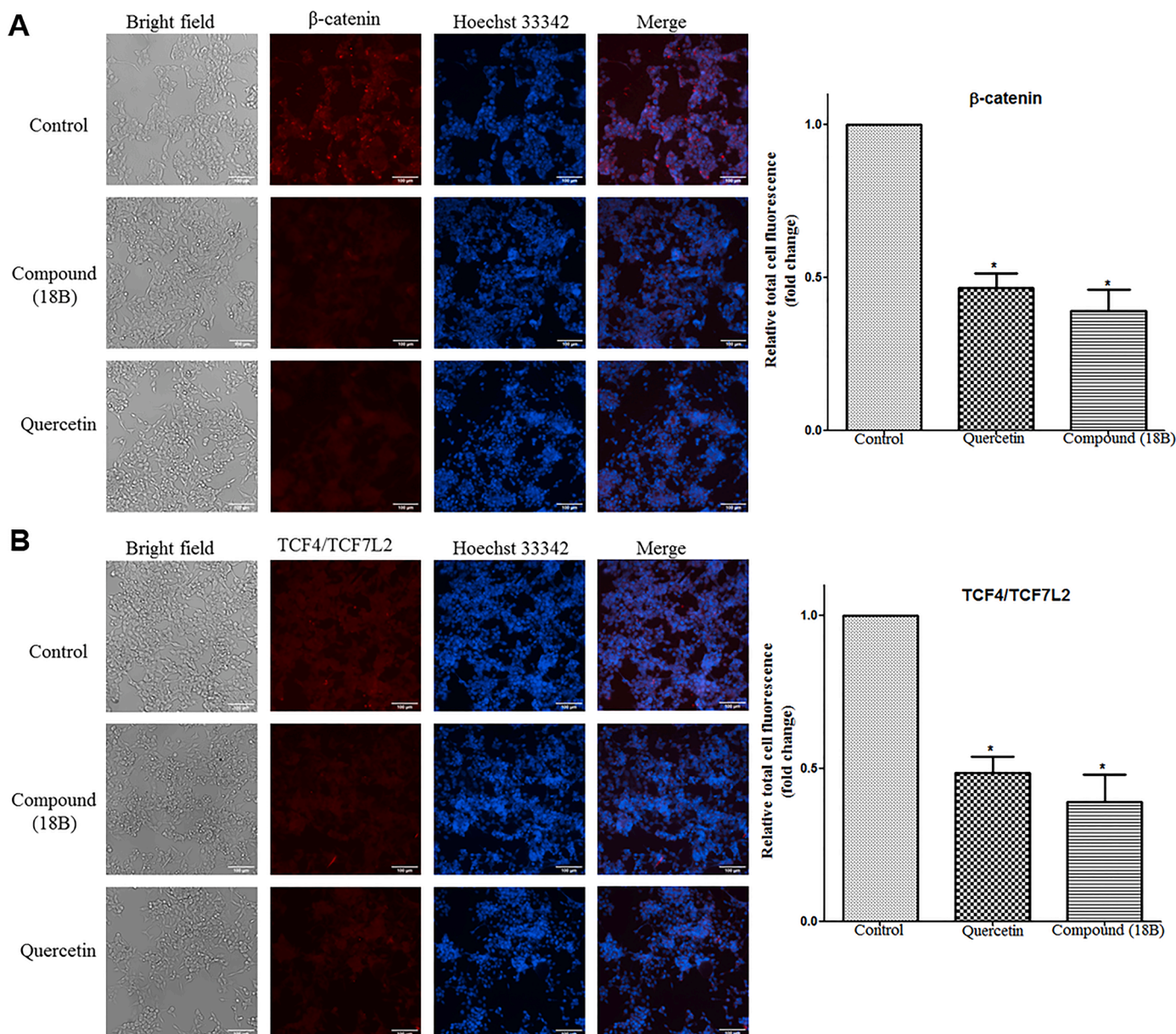


Fig. 9. Effect of compound (18B) on β -catenin and TCF4 protein expression against HCT116 cells. Cells were treated with IC_{50} concentration of compound (18B) or quercetin for 24 hours. (A, B): The immunocytofluorescence results revealed that compound (18B) significantly downregulates β -catenin and TCF4 protein expression level. Results are expressed as mean \pm S.D.* $p < 0.05$ versus control. Magnification 20X and scale bar 100 μ m.

Structure-based evaluation of small molecules for β -catenin/TCF4 interaction inhibition

The crystal structure (PDB ID – 2GL7 and PDB ID – 1JPW) for active binding residues (Hot spot) on β -catenin which interacts with TCF4 from Gly13 to Asp23 region was analysed, to design β -catenin/TCF4 interaction inhibitors which are summarized in Table 1 and Fig. 4. The novel 4,7-disubstituted 8-methoxyquinazoline derivatives with drug-like properties were subsequently docked on β -catenin (PDB ID – 2GL7) using Autodock 4.2.6. The binding site interactions on β -catenin, estimated Gibbs free binding energy (ΔG), and predicted inhibitory constant (K_i) values are summarized in Table 2. These compounds showed interactions with the active site residues on β -catenin and thus capable of hindering the TCF4 binding, thereby disrupting β -catenin/TCF4 interactions.

Synthesis of compounds

The synthetic procedure for obtaining novel quinazoline core derivatives is illustrated in Scheme 1. 4-Acetoxy-3-methoxybenzoic acid (1) [77] was nitrated using nitrating mixture in acetic acid to offer the nitro derivative (2) [78]. The acetyl group got removed during the processing of the reaction mixture. The nitro derivative (2) was esterified with methanol and thionyl chloride to yield 3, which was treated with 3-bromochloropropane to obtain the desired ether derivative (4). Carboxylic group in 5, obtained by alkaline hydrolysis of the ester (4) was converted to the amide (6) by derivatizing it to chloro derivative with thionyl chloride followed by treatment with ammonia. The nitro group of compound (6) was reduced by iron/sodium chloride in methanolic solution to 7. Heating of compound (7) with formic acid yielded the cyclised product (8). Treatment of the quinazolinone (8) with thionyl chloride followed by substituted aniline derivatives offered the substituted 4-anilines (8-13). The targeted compounds (14A – 18C)

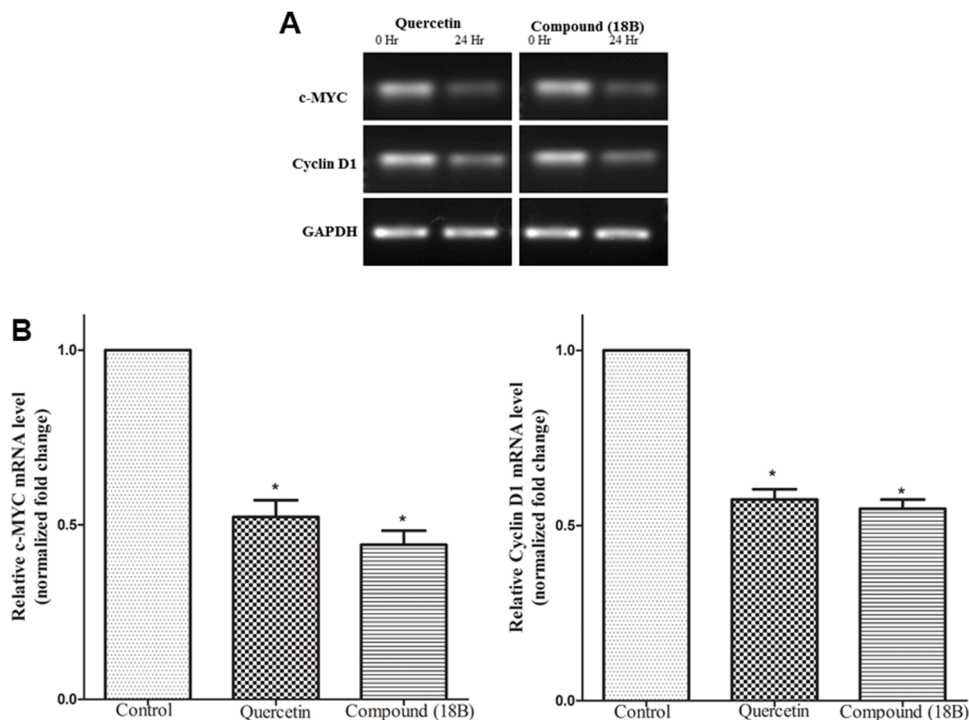


Fig. 10. Effect of compound (18B) on Wnt target genes against HCT116 cells. Cells were treated with IC₅₀ concentration of compound (18B) or quercetin for 24 hours. (A, B): Compound (18B) significantly downregulates mRNA levels of c-MYC and Cyclin D1. Results are expressed as mean ± S.D. * p < 0.05 versus control.

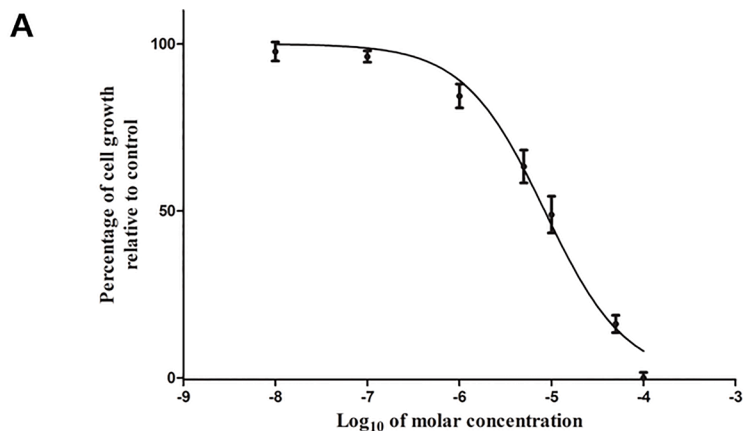
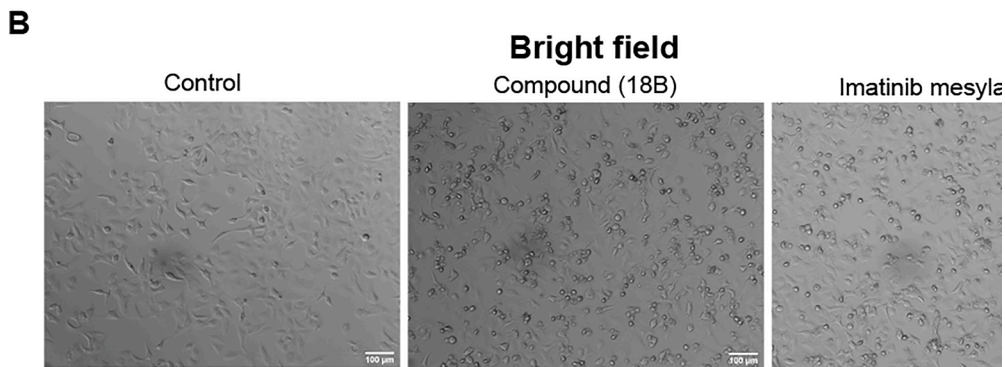


Fig. 11. Concentration response curve of compound (18B) against primary human gallbladder cancer cells. (A): Primary human gallbladder cancer cells were treated with compound (18B) at seven different concentration viz. 0.01, 0.1, 1, 5, 10, 50 and 100 μM for 48 hours and the concentration that caused a 50% reduction in cell growth (IC₅₀) relative to control (0.5% v/v DMSO treated) was determined by the SRB assay. Results are expressed as mean ± S.D. (B): Compound (18B) treated with IC₅₀ concentration induced morphological changes like membrane blebbing and cell shrinkage after 48 hours. Magnification 10X and scale bar 100 μm.



were obtained by substitution of the chloro group in the 4-aniline derivatives (**9–13**) with the desired cyclic amines in good yields. Spectral and elemental data of the synthesised compounds were in agreement with their assigned structures.

Cytotoxicity study using Sulforhodamine B (SRB) assay

All of the newly synthesized target compounds were evaluated for growth inhibitory activity against constitutively activated β -catenin/TCF4 signaling cancer cells [HCT116 (human colon cancer) and HepG2 (human liver cancer)] using the SRB assay. Cells were treated with the test compounds at seven different concentrations (0.01, 0.1, 1, 5, 10, 50 and 100 μ M) for 48 hours and the concentration that caused a 50 % reduction in cell growth (IC_{50}) relative to control (0.5% v/v DMSO treated) was determined. The IC_{50} values are summarized in Table 3. Cytotoxic potencies of these derivatives were found to be comparable with those of imatinib mesylate, which is clinically widely used anticancer drug for treating gastrointestinal cancers. Cytotoxic potencies (IC_{50}) of these derivatives ranged from 5.64 ± 0.68 to 23.18 ± 0.45 μ M against HCT116 and HepG2 cells. Notably, compound (**18B**) was found to be the most potent compound. The concentration response curves of compound (**18B**) against HCT116 and HepG2 cell lines are shown in Fig. 5.

A short SAR for these compounds has been framed because chemical modifications in the quinazoline scaffold have been carried out only at two positions, i.e. changing the cyclic amino group in the side chain at C₇ and substituting different aromatic groups at the nitrogen on C₄. Some generalisations are made here. All the synthesized compounds offered anticancer potencies in approximately the same range as offered by the clinically used drug imatinib against the two cancer cell lines. N-Methylpiperazine group in the side chain offered compounds (**15B**, **16B**, **17B** and **18B**) with superior activity over other compounds obtained by substituting morpholine or 1,2,4-triazole groups. Morpholine yielded more active compounds than the compounds obtained by substituting 1,2,4-triazole. A more hydrophobic group like benzyloxy (**17B**) or *m*-fluorobenzyloxy (**18B**) offered more potent compounds than *m*-chloro, *m*-bromo or *m*-chloro-*p*-fluoro groups. Both the compounds (**17B** and **18B**) offered superior anticancer activity than the standard drug imatinib against both the cancer cell lines. It is interesting to note that the molecular docking studies also indicated lower estimated Gibbs free binding energy (ΔG) and higher predicted potencies [predicted inhibition constant (K_i)] for these two compounds (**17B** and **18B**) over the remaining ones.

Compound (18B) induces morphological changes and apoptosis in HCT116 and HepG2 cells

Based on the *in vitro* cytotoxicity data, compound (**18B**), the most potent compound was selected for further biological evaluation. Apoptosis is a well-known process of programmed cell death [83]. Changes in apoptosis include membrane blebbing, cell shrinkage, nuclear fragmentation, chromatin condensation, global mRNA decay and chromosomal DNA fragmentation. We investigated the ability of compound (**18B**) to induce apoptosis in HCT116 and HepG2 cells after 48 hours incubation at its IC_{50} concentration. Morphological changes like membrane blebbing and cell shrinkage were observed with compound (**18B**) whereas control cells showed unaltered morphological changes as shown in Fig. 6. Control cells exhibited uniform dispersed nucleus whereas nuclear fragmentation and condensation were observed with compound (**18B**) when stained with Hoechst 33342 which confirmed the induction of apoptosis. Apoptosis is accompanied by loss of phospholipid membrane integrity resulting in exposure of phosphatidylserine (PS) on the outer surface of the cells [84]. Annexin V has a high affinity for PS whereas propidium iodide (PI) is a fluorescent DNA-staining dye permeable to cells with poor membrane integrity. Thus, annexin V and PI dual staining was used to distinguish viable

(annexin V⁻, PI⁻), early apoptotic (annexin V⁺, PI⁻), late apoptotic (annexin V⁺, PI⁺) and necrotic (annexin V⁻, PI⁺) cells. The percentage of early and late apoptotic cells after 48 hours incubation with compound (**18B**) at IC_{50} concentration were 14.5% and 35.2% respectively for HCT116 cells, whereas 18.7% and 34.4% respectively, for HepG2 cells as shown in Fig. 7.

Compound (18B) suppresses the migration in HCT116 and HepG2 cells

As migration is a crucial step for the process of metastasis, the effect of compound (**18B**) on inhibition of cell migration was studied. This assay mimics the cell migration process *in vivo* [85]. Compound (**18B**) significantly suppresses the migration as compared to control in HCT116 and HepG2 cells as shown in Fig. 7.

Compound (18B) downregulates β -catenin/TCF4 signaling pathway in HCT116 cells

Molecular docking results showed that compound (**18B**) interacted with the active site residues on β -catenin corresponding to TCF4 residues from Asp16 to Phe21. The estimated Gibbs free binding energy (ΔG) was found to be -9.4 kcal/mole and predicted K_i was 129.57 nM. Moreover, mutation to Ala or deletion of active binding residues on β -catenin showed reduction in binding with compound (**18B**) in molecular docking experiments which are summarized in supporting information Table S1. These observations indicated that compound (**18B**) was capable of hindering the TCF4 binding on β -catenin, thereby disrupting β -catenin/TCF4 interactions.

In order to determine the molecular mechanisms a cell-based TOP-Flash/FOPFlash assay was performed so as to examine whether compound (**18B**) can downregulate β -catenin/TCF4 mediated transcriptional activity. Quercetin, a known inhibitor of β -catenin/TCF4 signaling pathway was used as a reference standard [86]. It was observed that compound (**18B**) at its IC_{50} concentration significantly reduced TOP-luciferase activity by 41.66 ± 12.32 % while FOP-luciferase activity remained unaffected in HCT116 cells as shown in Fig. 8. This observation indicated that the transcriptional activity of β -catenin/TCF4 was inhibited by compound (**18B**) suggesting its inhibitory effect on the β -catenin/TCF4 signaling pathway.

Compound (18B) downregulates β -catenin and TCF4 protein expression in HCT116 cells

In order to understand whether suppression of β -catenin/TCF4 transcriptional activity by compound (**18B**) is mediated through the changes in protein expression of β -catenin and TCF4, the effect of compound (**18B**) was explored on their expression at the protein level by immunocytofluorescence as shown in Fig. 9. The immunocytofluorescence results revealed that the protein level of β -catenin and TCF4 was elevated in control HCT116 cells. Compound (**18B**) was found to significantly downregulate β -catenin and TCF4 protein expression levels.

Compound (18B) downregulates the expression of Wnt target genes in HCT116 cells

We investigated the effects of compound (**18B**) on Wnt target genes (like c-MYC and Cyclin D1). Compound (**18B**) significantly downregulates mRNA levels of c-MYC and Cyclin D1 as shown in Fig. 10. These observations revealed that the transcriptional activity of β -catenin/TCF4 was inhibited by compound (**18B**) and thus it downregulated β -catenin/TCF4 signaling pathway.

Evaluation of compound (18B) for its cytotoxic potential in primary human gallbladder cancer cell culture

Primary human gallbladder cancer cell culture was derived from surgically resected human GBC tissue specimen of a 60 year old male patient. Cultured tumour cells grew as an adherent monolayer with characteristic epithelial morphological features. Primary cell culture was used to evaluate the cytotoxicity of compound (18B) in human gallbladder cancer from SRB assay. The cytotoxic potential of compound (18B) (IC_{50} 8.50 ± 1.44 , Mean \pm S.D.) was found to be higher in comparison to imatinib mesylate (IC_{50} 15.56 ± 1.26 , Mean \pm S.D.) against primary human gallbladder cancer cells. Moreover at IC_{50} concentration we observed morphological changes like membrane blebbing and cell shrinkage after 48 hours, which are characteristic features of apoptosis as shown in Fig.11, suggesting its promising therapeutic potential against gallbladder cancer.

Conclusion

This study provides novel insights to design β -catenin/TCF4 interaction inhibitors for the discovery of small molecules targeting Wnt/ β -catenin pathway. The discovery of new potent inhibitors could provide a new class of therapeutic target and might be helpful for the management of cancer patients with dysregulated Wnt/ β -catenin signaling.

We focused on β -catenin active binding residues which interact with TCF4 from Gly13 to Asp23 region for designing β -catenin/TCF4 interaction inhibitors with the goal of overcoming over-activation of Wnt/ β -catenin signaling pathway. Molecular docking studies revealed that these compounds showed interactions with the active site residues on β -catenin and thus capable of hindering the TCF4 binding, thereby disrupting β -catenin/TCF4 interactions.

Fifteen compounds possessing 4,7-disubstituted 8-methoxyquinazoline core scaffold were synthesized. These novel quinazoline derivatives were identified as potential cytotoxic agents against constitutively activated β -catenin/TCF4 signaling cancer cells (HCT116 and HepG2) and were found to be comparable in potency with imatinib mesylate, a widely used clinical anti-cancer drug for the treating gastrointestinal cancers. Compound (18B), was identified as the most potent compound among the series. This new series of compounds could prove to be an important lead to obtain analogues with much higher potency and selectivity for cancer chemotherapy.

Compound (18B) induced apoptosis and inhibited cell migration against HCT116 and HepG2 cells. Mechanistic studies indicated that compound (18B) significantly downregulated β -catenin/TCF4 signaling pathway, β -catenin and TCF4 protein expression, and mRNA levels of c-MYC and Cyclin D1 against HCT116 cells and showed cytotoxicity against primary human gallbladder cancer cells. All these observations indicated that compound (18B) downregulated β -catenin/TCF4 signaling pathway and this could be one of the mechanisms by which it exerts its anticancer activity.

Till date there is not a single effective FDA approved drug as anti-cancer agent targeting the β -catenin/TCF4 signaling pathway. Compound (18B) has been found to be more potent cytotoxic agent than imatinib mesylate, a clinically widely used anti-cancer drug for treating gastrointestinal cancers. The adjuvant chemotherapeutic agents provide minimal benefits to gastrointestinal cancer patients and are also ineffective in eliminating the self-renewing cancer stem cells.

Compound (18B) represents a promising lead molecule and chemical probe as anticancer agent against colon, hepatocellular and gallbladder cancers targeting β -catenin/TCF4 signaling pathway, which could provide a new class of therapeutic agents targeting this pathway. Such agents could be helpful for the management of cancer patients with dysregulated Wnt/ β -catenin signaling, and overcoming the prevalence of drug resistance. But, it needs to be validated further in *in vivo* animal models of cancer

The present study has few limitations that need attention while

implicating the results to a specific context. The first limitation is the present study did not examine the binding affinities of the novel synthesized compounds on β -catenin and TCF4 interaction through experimental methods (fluorescence polarization assay or surface plasmon resonance or isothermal titration calorimetry) rather focused on virtual screening method (AutoDock). Another limitation is the present study did not examine the effects of compound (18B) on the apoptotic markers rather focused on determination of apoptosis induction through morphological changes using microscopic images and Flow Cytometric analysis. Future studies are required to study the efficacy and potency of compound (18B) in *in vivo* models.

Funding information

This research did not receive any specific grant from funding agencies in the public, commercial, or not-for-profit sectors.

CRediT authorship contribution statement

Kaushik Neogi: Conceptualization, Methodology, Data curation, Writing – original draft. **Prashant R. Murumkar:** Conceptualization. **Priyanshu Sharma:** . **Poonam Yadav:** . **Mallika Tewari:** Conceptualization. **Devarajan Karunakaran:** Conceptualization. **Prasanta Kumar Nayak:** Conceptualization. **Mange Ram Yadav:** Conceptualization.

Declaration of Competing Interest

The authors declare no conflict of interest.

Acknowledgment

Kaushik Neogi would like to thank Indian Institute of Technology (Banaras Hindu University), Varanasi and Ministry of Human Resource and Development (MHRD), New Delhi, India, for the teaching assistantship.

Supplementary materials

Supplementary material associated with this article can be found, in the online version, at doi:10.1016/j.tranon.2022.101395.

References

- [1] World Health Organization, Cancer (2018). Cancer, <https://www.who.int/news-room/fact-sheets/detail/cancer>. accessed 18th July 2021.
- [2] B.N. Ames, L.S. Gold, W.C. Willett, The causes and prevention of cancer, Proc. Natl. Acad. Sci. 92 (1995) 5258–5265, <https://doi.org/10.1073/pnas.92.12.5258>.
- [3] C.Y. Logan, R. Nusse, The Wnt signaling pathway in development and disease, Annu. Rev. Cell Dev. Biol. 20 (2004) 781–810, <https://doi.org/10.1146/annurev.cellbio.20.010403.113126>.
- [4] T. Grigoryan, P. Wend, A. Klaus, W. Birchmeier, Deciphering the function of canonical Wnt signals in development and disease: conditional loss-and gain-of-function mutations of β -catenin in mice, Genes Dev. 22 (2008) 2308–2341, <https://doi.org/10.1101/gad.1686208>.
- [5] H. Clevers, Wnt/ β -catenin signaling in development and disease, Cell 127 (2006) 469–480, <https://doi.org/10.1016/j.cell.2006.10.018>.
- [6] T. Reya, H. Clevers, Wnt signalling in stem cells and cancer, Nature 434 (2005) 843–850, <https://doi.org/10.1038/nature03319>.
- [7] R. Nusse, H. Clevers, Wnt/ β -catenin signaling, disease, and emerging therapeutic modalities, Cell 169 (2017) 985–999, <https://doi.org/10.1016/j.cell.2017.05.016>.
- [8] L. Thorstensen, R.A. Lothe, The WNT signaling pathway and its role in human solid tumors, Atlas Genetic. Cytogenetic. Oncol. Haematol. 7 (2003) 146–161, <https://doi.org/10.4267/2042/37975>.
- [9] D.V. Tauriello, I. Jordens, K. Kirchner, J.W. Slootstra, T. Kruitwagen, B. A. Bouwman, M. Noutsou, S.G. Rüdiger, K. Schwamborn, A. Schambony, Wnt/ β -catenin signaling requires interaction of the dishevelled DEP domain and C terminus with a discontinuous motif in Frizzled, Proc. Natl. Acad. Sci. 109 (2012) E812–E820, <https://doi.org/10.1073/pnas.1114802109>.
- [10] O. Bernatik, R.S. Ganji, J.P. Dijksterhuis, P. Konik, I. Cervenka, T. Polonio, P. Krejci, G. Schulte, V. Bryja, Sequential activation and inactivation of dishevelled in the Wnt/ β -catenin pathway by casein kinases, J. Biol. Chem. 286 (2011) 10396–10410, <https://doi.org/10.1074/jbc.M110.169870>.

- [11] B.T. MacDonald, X. He, Frizzled and LRP5/6 receptors for Wnt/ β -catenin signaling, *Cold Spring Harbor perspectives in biology*, 4 (2012) 1-23. <https://doi.org/10.1101/cshperspect.a007880>.
- [12] X. Zeng, K. Tamai, B. Doble, S. Li, H. Huang, R. Habas, H. Okamura, J. Woodgett, X. He, A dual-kinase mechanism for Wnt co-receptor phosphorylation and activation, *Nature* 438 (2005) 873–877, <https://doi.org/10.1038/nature04185>.
- [13] B.T. MacDonald, K. Tamai, X. He, Wnt/ β -catenin signaling: components, mechanisms, and diseases, *Dev. Cell* 17 (2009) 9–26, <https://doi.org/10.1016/j.devcel.2009.06.016>.
- [14] R. Stadeli, R. Hoffmann, K. Basler, Transcription under the control of nuclear Arm/ β -catenin, *Curr. Biol.* 16 (2006) 378–385, <https://doi.org/10.1016/j.cub.2006.04.019>.
- [15] H.C. Jung, K. Kim, Identification of MYCBP as a β -catenin/LEF-1 target using DNA microarray analysis, *Life Sci.* 77 (2005) 1249–1262, <https://doi.org/10.1016/j.lfs.2005.02.009>.
- [16] T.C. He, A.B. Sparks, C. Rago, H. Hermeking, L. Zawel, L.T. Da Costa, P.J. Morin, B. Vogelstein, K.W. Kinzler, Identification of c-MYC as a target of the APC pathway, *Science* 281 (1998) 1509–1512, <https://doi.org/10.1126/science.281.5382.1509>.
- [17] O. Tetsu, F. McCormick, β -Catenin regulates expression of cyclin D1 in colon carcinoma cells, *Nature* 398 (1999) 422–426, <https://doi.org/10.1038/18884>.
- [18] T. Zhang, T. Otevrel, Z. Gao, Z. Gao, S.M. Ehrlich, J.Z. Fields, B.M. Boman, Evidence that APC regulates survivin expression, *Cancer Res.* 61 (2001) 8664–8667.
- [19] B. Mann, M. Gelos, A. Siedow, M. Hanski, A. Gratchev, M. Ilyas, W. Bodmer, M. Moyer, E. Riecken, H. Buhr, Target genes of β -catenin-T cell-factor/lymphoid-enhancer-factor signaling in human colorectal carcinomas, *Proc. Natl. Acad. Sci.* 96 (1999) 1603–1608, <https://doi.org/10.1073/pnas.96.4.1603>.
- [20] E.M. Boon, R. van der Neut, M. van de Wetering, H. Clevers, S.T. Pals, Wnt signaling regulates expression of the receptor tyrosine kinase met in colorectal cancer, *Cancer Res.* 62 (2002) 5126–5128.
- [21] T.C. He, T.A. Chan, B. Vogelstein, K.W. Kinzler, PPAR δ is an APC-regulated target of nonsteroidal anti-inflammatory drugs, *Cell* 99 (1999) 335–345, [https://doi.org/10.1016/S0092-8674\(00\)81664-5](https://doi.org/10.1016/S0092-8674(00)81664-5).
- [22] E.K.L. Neufeld, Novel double-negative feedback loop between adenomatous polyposis coli and Musashi1 in colon epithelia, *J. Biol. Chem.* 286 (2011) 4946–4950, <https://doi.org/10.1074/jbc.C110.205922>.
- [23] B. Wu, S.P. Crampton, C.C. Hughes, Wnt signaling induces matrix metalloproteinase expression and regulates T cell transmigration, *Immunity* 26 (2007) 227–239, <https://doi.org/10.1016/j.immuni.2006.12.007>.
- [24] T. Brabletz, A. Jung, S. Dag, F. Hlubek, T. Kirchner, β -Catenin regulates the expression of the matrix metalloproteinase-7 in human colorectal cancer, *Am. J. Pathol.* 155 (1999) 1033–1038, [https://doi.org/10.1016/S0002-9440\(10\)65204-2](https://doi.org/10.1016/S0002-9440(10)65204-2).
- [25] G.N. Marchenko, N.D. Marchenko, L. Jay, A.Y. Strongin, Promoter characterization of the novel human matrix metalloproteinase-26 gene: regulation by the T-cell factor-4 implies specific expression of the gene in cancer cells of epithelial origin, *Biochem. J.* 363 (2002) 253–262, <https://doi.org/10.1042/0264-6021:3630253>.
- [26] X. Zhang, J.P. Gaspard, D.C. Chung, Regulation of vascular endothelial growth factor by the Wnt and K-ras pathways in colonic neoplasia, *Cancer Res.* 61 (2001) 6050–6054.
- [27] T.H. Kim, H. Xiong, Z. Zhang, B. Ren, β -Catenin activates the growth factor endothelin-1 in colon cancer cells, *Oncogene* 24 (2005) 597–604, <https://doi.org/10.1038/sj.onc.1208237>.
- [28] C. Liu, Y. Li, M. Semenov, C. Han, G.-H. Baeg, Y. Tan, Z. Zhang, X. Lin, X. He, Control of β -catenin phosphorylation/degradation by a dual-kinase mechanism, *Cell* 108 (2002) 837–847, [https://doi.org/10.1016/S0092-8674\(02\)00685-2](https://doi.org/10.1016/S0092-8674(02)00685-2).
- [29] T.P. Rao, M. Kuhl, An updated overview on Wnt signaling pathways, *Circ. Res.* 106 (2010) 1798–1806, <https://doi.org/10.1161/CIRCRESAHA.110.219840>.
- [30] H. Suzuki, D.N. Watkins, K.W. Jair, K.E. Schuebel, S.D. Markowitz, W.D. Chen, T. P. Pretlow, B. Yang, Y. Akiyama, M. Van Engeland, Epigenetic inactivation of SFRP genes allows constitutive Wnt signaling in colorectal cancer, *Nat. Genet.* 36 (2004) 417–422, <https://doi.org/10.1038/ng1330>.
- [31] B. Mann, A. Gratchev, E. Riede, I. Schmidt-Wolf, B. Trojanek, P. Moyer, C. Hanski, H. Buhr, Beta-catenin overexpression in metastasized colorectal carcinoma—an important mechanism in progression of the disease?, *Langenbecks Archiv fur Chirurgie. Supplement. Kongressband. Deutsche Gesellschaft fur Chirurgie, Kongress (1998)* 303–306.
- [32] Z. Chen, X. He, M. Jia, Y. Liu, D. Qu, D. Wu, P. Wu, C. Ni, Z. Zhang, J. Ye, J. Xu, J. Huang, β -catenin overexpression in the nucleus predicts progress disease and unfavourable survival in colorectal cancer: a meta-analysis, *PLoS One* 8 (2013) 1–9, <https://doi.org/10.1371/journal.pone.0063854>.
- [33] B.M. Bush, A.T. Brock, J.A. Deng, R.A. Nelson, T.F. Sumter, The Wnt/ β -catenin/TCF-4 pathway upregulates HMGA1 expression in colon cancer, *Cel. Biochemistry and function*, 31 (2013) 228–236. <https://doi.org/10.1002/cbf.2876>.
- [34] M. van de Wetering, E. Sancho, C. Verweij, W. de Lau, I. Oving, A. Hurlstone, K. van der Horn, E. Battle, D. Coudreuse, A.-P. Haramis, M. Tjon-Pon-Fong, P. Moerer, M. van den Born, G. Soete, S. Pals, M. Eilers, R. Medema, H. Clevers, The β -Catenin/TCF-4 Complex Imposes a Crypt Progenitor Phenotype on Colorectal Cancer Cells, *Cell* 111 (2002) 241–250, [https://doi.org/10.1016/S0092-8674\(02\)01014-0](https://doi.org/10.1016/S0092-8674(02)01014-0).
- [35] L.J. Liu, S.X. Xie, Y.T. Chen, J.L. Xue, C.J. Zhang, F. Zhu, Aberrant regulation of Wnt signaling in hepatocellular carcinoma, *World J. Gastroenterol.* 22 (2016) 7486–7499, <https://doi.org/10.3748/wjg.v22.i33.7486>.
- [36] A. Bengochea, M.M. de Souza, L. Lefrancois, E. Le Roux, O. Galy, I. Chemin, M. Kim, J.R. Wands, C. Trepo, P. Hainaut, J.Y. Scoazec, L. Vitvitski, P. Merle, Common dysregulation of Wnt/Frizzled receptor elements in human hepatocellular carcinoma, *Br. J. Cancer* 99 (2008) 143–150, <https://doi.org/10.1038/sj.bjc.6604422>.
- [37] H.C. Lee, M. Kim, J.R. Wands, Wnt/Frizzled signaling in hepatocellular carcinoma, *Front. Biosci.* 11 (2006) 1901–1915, <https://doi.org/10.2741/1933>.
- [38] K.N. Nejak Bowen, S.P. Monga, Beta-catenin signaling, liver regeneration and hepatocellular cancer: sorting the good from the bad, *Semin. Cancer Biol.* 21 (2011) 44–58, <https://doi.org/10.1016/j.semcancer.2010.12.010>.
- [39] D.H. Zhao, J.J. Hong, S.Y. Guo, R.L. Yang, J. Yuan, C.J. Wen, K.Y. Zhou, C.J. Li, Aberrant expression and function of TCF4 in the proliferation of hepatocellular carcinoma cell line BEL-7402, *Cell Res.* 14 (2004) 74–80, <https://doi.org/10.1038/sj.cr.7290205>.
- [40] Y. Takigawa, A. Brown, Wnt signaling in liver cancer, *Curr. Drug Targets* 9 (2008) 1013–1024, <https://doi.org/10.2174/138945008786786127>.
- [41] M.D. Thompson, S.P. Monga, Wnt/ β -catenin signaling in liver health and disease, *Hepatology* 45 (2007) 1298–1305, <https://doi.org/10.1002/hep.21651>.
- [42] W.S. Moon, H.S. Park, H. Lee, R. Pai, A.S. Tarnawski, K.R. Kim, K.Y. Jang, Co-Expression of Cox-2, C-Met and β -catenin in Cells Forming Invasive front of Gallbladder Cancer, *Cancer Res. Treat.* 37 (2005) 171–176, <https://doi.org/10.4143/crt.2005.37.3.171>.
- [43] D. Zhang, Y. Wang, Y. Dai, J. Wang, T. Suo, H. Pan, H. Liu, S. Shen, H. Liu, CIZ1 promoted the growth and migration of gallbladder cancer cells, *Tumor Biology* 36 (2015) 2583–2591, <https://doi.org/10.1007/s13277-014-2876-y>.
- [44] Y. Kimura, T. Furuhashi, M. Mukaiya, C. Kihara, M. Kawakami, K. Okita, Y. Yanai, H. Zenbutsu, M. Satoh, S. Ichimiya, Frequent beta-catenin alteration in gallbladder carcinomas, *J. Exp. Clin. Cancer Res.* 22 (2003) 321–328.
- [45] H.J. Chang, C. Do Jee, W.H. Kim, Mutation and altered expression of β -catenin during gallbladder carcinogenesis, *Am. J. Surg. Pathol.* 26 (2002) 758–766, <https://doi.org/10.1097/00000478-200206000-00009>.
- [46] M. Ghosh, P. Sakhuja, S. Singh, A.K. Agarwal, p53 and beta-catenin expression in gallbladder tissues and correlation with tumor progression in gallbladder cancer, *Saudi J. Gastroenterol.* 19 (2013) 34–39, <https://doi.org/10.4103/1319-3767.105922>.
- [47] D.S.K. Chandrawati, S. Mitra, Beta-catenin expression in gallbladder tissues and its role in carcinogenesis and tumor progression in gallbladder carcinoma, *J. Med. Sci. Clin. Res.* 6 (2018) 591–599.
- [48] H. Puhalla, B. Herberger, A. Soleiman, M. Filipits, F. Laengle, T. Gruenberger, F. Wrba, E-cadherin and β -catenin expression in normal, inflamed and cancerous gallbladder tissue, *Anticancer Res.* 25 (2005) 4249–4254.
- [49] M. Fasolini, X. Wu, M. Flocco, J.-Y. Trosset, U. Oppermer, S. Knapp, Hot spots in Tcf4 for the interaction with β -catenin, *J. Biol. Chem.* 278 (2003) 21092–21098, <https://doi.org/10.1074/jbc.M301781200>.
- [50] J.P. von Kries, G. Winbeck, C. Asbrand, T. Schwarz-Romond, N. Sochnikova, A. Dell’Oro, J. Behrens, W. Birchmeier, Hot spots in β -catenin for interactions with LEF-1, *conductin and APC*, *Nat. Struct. Biol.* 7 (2000) 800–807, <https://doi.org/10.1038/79039>.
- [51] F. Poy, M. Lepourcelet, R.A. Shivdasani, M.J. Eck, Structure of a human Tcf4- β -catenin complex, *Nat. Struct. Biol.* 8 (2001) 1053–1057, <https://doi.org/10.1038/nsb720>.
- [52] R.D. Taylor, P.J. Jewsbury, J.W. Essex, A review of protein-small molecule docking methods, *J. Comput. Aided Mol. Des.* 16 (2002) 151–166, <https://doi.org/10.1023/a:1020155510718>.
- [53] I.D. Kuntz, E.C. Meng, B.K. Shoichet, Structure-based molecular design, *Acc. Chem. Res.* 27 (1994) 117–123, <https://doi.org/10.1021/ar00041a001>.
- [54] L.W. Hardy, A. Malikyil, The impact of structure-guided drug design on clinical agents, *Curr. Drug Discov* 3 (2003) 15–20.
- [55] D. Prada-Gracia, S. Huerta-Yepez, L.M. Moreno-Vargas, Application of computational methods for anticancer drug discovery, design, and optimization, *Boletın Medico Del Hospital Infantil de Mexico (English Edition)* 73 (2016) 411–423, <https://doi.org/10.1016/j.bmhmx.2016.10.006>.
- [56] E.R. Wood, A.T. Truesdale, O.B. McDonald, D. Yuan, A. Hassell, S.H. Dickerson, B. Ellis, C. Pennisi, E. Horne, K. Lackey, A unique structure for epidermal growth factor receptor bound to GW572016 (Lapatinib): relationships among protein conformation, inhibitor off-rate, and receptor activity in tumor cells, *Cancer Res.* 64 (2004) 6652–6659, <https://doi.org/10.1158/0008-5472.CAN-04-1168>.
- [57] M. Mohamed, J. Graham, P. Kirkpatrick, Gefitinib, *Nature Reviews, Cancer* 3 (2003) 556–557, <https://doi.org/10.1038/nrc1159>.
- [58] J. Dowell, J.D. Minna, P. Kirkpatrick, Erlotinib hydrochloride, *Nat. Rev. Drug Discovery* 4 (2005) 13–14, <https://doi.org/10.1038/nrd1612>.
- [59] V. Nelson, J. Ziehr, M. Agulnik, M. Johnson, Afatinib: emerging next-generation tyrosine kinase inhibitor for NSCLC, *OncoTarget. Therapy* 6 (2013) 135–143, <https://doi.org/10.2147/OTT.S23165>.
- [60] B. Moy, P. Kirkpatrick, S. Kar, P. Goss, Lapatinib, *Nature reviews drug discovery*, 6 (2007) 431–432. <https://doi.org/10.1038/nrd2332>.
- [61] M.W. Sim, M.S. Cohen, The discovery and development of vandetanib for the treatment of thyroid cancer, *Expert Opin. Drug Discov.* 9 (2014) 105–114, <https://doi.org/10.1517/17460441.2014.866942>.
- [62] K.G. Petrov, Y.-M. Zhang, M. Carter, G.S. Cockerill, S. Dickerson, C.A. Gauthier, Y. Guo, R.A. Mook Jr, D.W. Rusnak, A.L. Walker, Optimization and SAR for dual ErbB-1/ErbB-2 tyrosine kinase inhibition in the 6-furanylquinazoline series, *Bioorg. Med. Chem. Lett.* 16 (2006) 4686–4691, <https://doi.org/10.1016/j.bmcl.2006.05.090>.
- [63] R. Morphy, Selectively nonselective kinase inhibition: striking the right balance, *J. Med. Chem.* 53 (2010) 1413–1437, <https://doi.org/10.1021/jm901132v>.
- [64] A.J. Barker, K.H. Gibson, W. Grundy, A.A. Godfrey, J.J. Barlow, M.P. Healy, J. R. Woodburn, S.E. Ashton, B.J. Curry, L. Scarlett, Studies leading to the identification of ZD1839 (IressaTM): an orally active, selective epidermal growth

- factor receptor tyrosine kinase inhibitor targeted to the treatment of cancer, *Bioorg. Med. Chem. Lett.* 11 (2001) 1911–1914, [https://doi.org/10.1016/s0960-894x\(01\)00344-4](https://doi.org/10.1016/s0960-894x(01)00344-4).
- [65] X. Wu, M. Li, Y. Qu, W. Tang, Y. Zheng, J. Lian, M. Ji, L. Xu, Design and synthesis of novel Gefitinib analogues with improved anti-tumor activity, *Bioorg. Med. Chem.* 18 (2010) 3812–3822, <https://doi.org/10.1016/j.bmc.2010.04.046>.
- [66] A.M. Venkatesan, C. Dehnhardt, Z. Chen, O. Dos Santos, E.D. Santos, K. Curran, S. Ayral-Kaloustian, L. Chen, Amino-substituted quinazoline derivatives as inhibitors of beta-catenin/tcf-4 pathway and cancer treatment agents, *Google Patents* (2009). <https://patents.google.com/patent/WO2008086462A3/en>.
- [67] C.M. Dehnhardt, A.M. Venkatesan, Z. Chen, S. Ayral-Kaloustian, O. Dos Santos, E. Delos Santos, K. Curran, M.T. Follettie, V. Diesl, J. Lucas, Design and synthesis of novel diaminoquinazolines with in vivo efficacy for β -catenin/T-cell transcriptional factor 4 pathway inhibition, *J. Med. Chem.* 53 (2010) 897–910, <https://doi.org/10.1021/jm901370m>.
- [68] Z. Chen, A.M. Venkatesan, C.M. Dehnhardt, O. Dos Santos, E.D. Santos, S. Ayral-Kaloustian, L. Chen, Y. Geng, K.T. Arndt, J. Lucas, 2, 4-Diamino-quinazolines as inhibitors of β -catenin/TCF-4 pathway: potential treatment for colorectal cancer, *Bioorg. Med. Chem. Lett.* 19 (2009) 4980–4983, <https://doi.org/10.1016/j.bmcl.2009.07.070>.
- [69] Y. Mao, N. Lin, W. Tian, X. Han, X. Han, Z. Huang, J. An, Design, synthesis, and biological evaluation of new diaminoquinazolines as β -catenin/Tcf4 pathway inhibitors, *J. Med. Chem.* 55 (2012) 1346–1359, <https://doi.org/10.1021/jm201494a>.
- [70] Y. Li, W. Lu, S.K. Saini, O. Moukha-Chafiq, V. Pathak, S. Ananthan, Identification of quinazoline compounds as novel potent inhibitors of Wnt/ β -catenin signaling in colorectal cancer cells, *Oncotarget* 7 (2016) 11263–11270, <https://doi.org/10.18632/oncotarget.7019>.
- [71] G.M. Morris, R. Huey, W. Lindstrom, M.F. Sanner, R.K. Belew, D.S. Goodsell, A. J. Olson, AutoDock4 and AutoDockTools4: automated docking with selective receptor flexibility, *J. Comput. Chem.* 30 (2009) 2785–2791, <https://doi.org/10.1002/jcc.21256>.
- [72] S. Forli, R. Huey, M.E. Pique, M.F. Sanner, D.S. Goodsell, A.J. Olson, Computational protein–ligand docking and virtual drug screening with the AutoDock suite, *Nat. Protoc.* 11 (2016) 905–919, <https://doi.org/10.1038/nprot.2016.051>.
- [73] J. Sampietro, C.L. Dahlberg, U.S. Cho, T.R. Hinds, D. Kimelman, W. Xu, Crystal structure of a β -catenin/BCL9/Tcf4 complex, *Mol. Cell* 24 (2006) 293–300, <https://doi.org/10.1016/j.molcel.2006.09.001>.
- [74] T.A. Graham, C. Weaver, F. Mao, D. Kimelman, W. Xu, Crystal structure of a β -catenin/Tcf complex, *Cell* 103 (2000) 885–896, [https://doi.org/10.1016/s0092-8674\(00\)00192-6](https://doi.org/10.1016/s0092-8674(00)00192-6).
- [75] PPCheck, A webserver for identification of non-covalent interactions at the interface of a protein-protein complex, <http://caps.ncbs.res.in/ppcheck/> (accessed 24 September 2017).
- [76] A. Sukhwal, R. Sowdhamini, Oligomerisation status and evolutionary conservation of interfaces of protein structural domain superfamilies, *Mol. Biosyst.* 9 (2013) 1652–1661, <https://doi.org/10.1039/c3mb25484d>.
- [77] A. Wissner, M.B. Floyd, S.K. Rabindran, R. Nilakantan, L.M. Greenberger, R. Shen, Y.-F. Wang, H.-R. Tsou, Syntheses and EGFR and HER-2 kinase inhibitory activities of 4-anilinoquinoline-3-carbonitriles: analogues of three important 4-anilinoquinazolines currently undergoing clinical evaluation as therapeutic antitumor agents, *Bioorg. Med. Chem. Lett.* 12 (2002) 2893–2897, [https://doi.org/10.1016/s0960-894x\(02\)00598-x](https://doi.org/10.1016/s0960-894x(02)00598-x).
- [78] J. Boyer, J. Morgan, L. Condensation of 3-Aminoquinones with o-Phenylenediamine, *J. Org. Chem.* 26 (1961) 1654–1656, <https://doi.org/10.1021/jo01064a619>.
- [79] P. Skehan, R. Storeng, D. Scudiero, A. Monks, J. McMahon, D. Vistica, J.T. Warren, H. Bokesch, S. Kenney, M.R. Boyd, New colorimetric cytotoxicity assay for anticancer-drug screening, *J. Natl. Cancer Inst.* 82 (1990) 1107–1112, <https://doi.org/10.1093/jnci/82.13.1107>.
- [80] V. Vichai, K. Kirtikara, Sulforhodamine B colorimetric assay for cytotoxicity screening, *Nat. Protoc.* 1 (2006) 1112–1116, <https://doi.org/10.1038/nprot.2006.179>.
- [81] C.C. Liang, A.Y. Park, J.L. Guan, In vitro scratch assay: a convenient and inexpensive method for analysis of cell migration in vitro, *Nat. Protoc.* 2 (2007) 329–333, <https://doi.org/10.1038/nprot.2007.30>.
- [82] M.T. Veeman, D.C. Slusarski, A. Kaykas, S.H. Louie, R.T. Moon, Zebrafish prickle, a modulator of noncanonical Wnt/Fz signaling, regulates gastrulation movements, *Curr. Biol.* 13 (2003) 680–685, [https://doi.org/10.1016/s0960-9822\(03\)00240-9](https://doi.org/10.1016/s0960-9822(03)00240-9).
- [83] S. Elmore, Apoptosis: a review of programmed cell death, *Toxicol. Pathol.* 35 (2007) 495–516, <https://doi.org/10.1080/01926230701320337>.
- [84] G. Koopman, C. Reutelingsperger, G. Kuijten, R. Keehnen, S. Pals, M. Van Oers, Annexin V for flow cytometric detection of phosphatidylserine expression on B cells undergoing apoptosis, *Blood* 84 (1994) 1415–1420, <https://doi.org/10.1182/blood.V84.5.1415.1415>.
- [85] L.G. Rodriguez, X. Wu, J.-L. Guan, J.-L. Guan, Wound-Healing Assay, in: *Cell Migration. Methods in Molecular Biology*, 294, Humana Press, Totowa, NJ, 2005, pp. 23–29, <https://doi.org/10.1385/1-59259-860-9:023>.
- [86] C.H. Park, J.Y. Chang, E.R. Hahm, S. Park, H.K. Kim, C.H. Yang, Quercetin, a potent inhibitor against β -catenin/Tcf signaling in SW480 colon cancer cells, *Biochem. Biophys. Res. Commun.* 328 (2005) 227–234, <https://doi.org/10.1016/j.brc.2004.12.151>.